

# Chapter 2 Paleoclimate of China

## 2.1 Introduction

The regional climate of China in the past can be studied by analyzing proxy data and modeling. In the last several decades, a plenty of proxy data, such as tree-rings, ice cores, stalagmite, peat, pollens, lake sediments, and historical documents were used by Chinese scientists to study climate changes of China. A longer perspective on climatic variability can be obtained by the study of natural evidences that are climate-dependent. Such evidences provide the proxy record of climate and are the foundation of paleoclimate studies. Thus, reconstructed paleoclimatic data from the proxy data provide the basis for studying the regional climate change of China at different time scales.

Many natural systems are dependent on climate; where evidence of such systems in the past still exists, it may be possible to derive paleoclimatic information from them. By definition, such proxy records of climate all contain a climatic signal, but the signal may be relatively weak, embedded in a great deal of extraneous “noise” arising from the effects of other (non-climatic) influences. The proxy material has acted as a filter, transforming climatic conditions at a point in time, or over a period, into a more or less permanent record, but the record is complex and incorporates other signals that may be irrelevant to the paleoclimatologist.

To extract the paleoclimatic signal from proxy data, we have to understand how, and to what extent, proxy materials are climate-dependent by using modern climatic records and proxy materials. Generally, we can assume that the modern relationships observed have operated, unchanged, throughout the period of interest (the principle of uniformitarianism). All paleoclimatic research, therefore, must build on studies of climate dependency in natural phenomena at the present. Dendroclimatic studies, for example, have benefited from a wealth of research into climate-tree growth relationships, which have enabled dendroclimatic models to be based on sound ecological principles. Significant advances have also been made in playnological research by improvements in our understanding of the relationships between modern climate and pollen rain. It is apparent, therefore,

that an adequate modern database and understanding of contemporary processes in the climate system are important prerequisites for reliable paleoclimatic reconstructions. However, not all environmental conditions in the past are represented in the period of modern experience. We must be aware of the possibility that erroneous paleoclimatic reconstructions may result from the use of modern climate-proxy data relationships when past conditions have no analog in the modern world.

For extending the climate series, calibration and assimilation are important in the reconstruction of the climate series for the past climate research in regional climate of China. The ice cores, tree-rings, stalagmite and documentary data have been used to estimate the regional temperature anomalies and precipitation to fill the gaps in observational series. As the Tibetan Plateau play a very important role in the climate of China, using more proxy data, mainly ice cores and tree rings from the Plateau, is necessary. A fundamental understanding of the climate change of China in the past is very valuable for understanding and detecting present and future climate change in China.

As a numerical tool, climate model has been used to estimate the spatial and temporal pattern of climate changes in the past. Models are used to test hypotheses about the causes of environmental changes in the past, to quantify the relative importance of one factor compared to another, and to examine the sensitivity of the climate system to different forcing mechanisms. Therefore, paleoclimatic modeling can provide the essential understanding of climate system variability, and its relation to both forcing mechanisms and feedbacks, which may amplify or reduce the direct consequences of particular forcing. Paleo-environmental data and modeling can help us to evaluate known climate changes in the past, and to comprehend the feedbacks and system responses that are of direct relevance to the understanding of the future impact of human activities.

## **2.2 Reconstructed climate of China**

Chinese climatologist Zhu Kezhen, published the first paper “Climate change during the historical time in China” on the climate change in China in 1925. Then Zhu published “Preliminary study on climate change during the last five thousand years in China” in 1972. In the last 50 years, more paleoclimate studies based on the different kinds of proxy data, such as ice cores, tree-rings, lake sediments, and varve records, have been made and have greatly improved our understanding to the paleoclimate of China. By use of the proxy data we can reconstruct precipitation and temperature

time series with various resolutions for long time. From these reconstructions we have known more climate change of China in the past.

One of the hot points in paleoclimate is abrupt climate change. A great deal of the evidences showed that there were series of abrupt change events in China in the Holocene since Younger Dryas. The assorted evidences indicate that the most of the cold periods identified in China correspond to those of the world. Discrepancy in timing may relate to the uncertainty in those and the Chinese series.

Two typical cold periods were found as abrupt climate changes at 8.2 kaBP (Wang N L et al., 2002) and at 4.0 kaBP in the Holocene. The later one is possible related to the collapses of ancient civilization in the Nile Valley and the Mesopotamia and the alternation of the ancient cultures in China. (Wang S W et al, 2004). The results of studies indicate that the collapses of ancient civilization in the world were associated with an abrupt shift to a cold and drought climate (Group of experts, 2000). The changes of wetness in Qinghai Lake are related well to the reduction of precipitation at 4.0 kaBP.

The occurrence of MWP (Mediaeval Warm Period, AD 900~1300) in China is also an important topic in the studies of historical climate changes. Zhang De'er (1994) has shown that the 13th century was a warm period during the last millennium. Wang et al. (2001) reconstructed the temperature series for eastern and western China with 50-year time resolution. The mean temperature from AD 850 to 1300 was about 0.2°C higher than the mean during the whole period except in the 12th century in eastern China. However, no prolonged warm period was found in western China from AD 900 to AD 1300. Therefore, the MWP can probably be traced only in eastern but not in western China. Ge et al. (2002) have synthesized the pollen, varve, stalagmite and documentary data, and indicated that there was a warm period from 930 to 1310, but the climate of 1110-1190 was colder than that of 1951-1980. A recent study on the stalagmite record in Beijing supports the suggestion that there was a warm climate during AD 900-1300 while temperature was 0.5°C higher than the present (Tan et al. 2003). Yang et al. (2002) examined the temperatures over the Tibetan Plateau based on the lake sediment, ice cores, tree-rings, peat, and glacier data. They found that the warmest period appeared before AD 1000 over the northeastern, but no warm period before AD 1300 over the western Tibetan Plateau. The climate was warm during AD 1150-1350 over the southern Tibetan Plateau.

Lin et al. (1990, 1995) and Wang (1990) have extended the temperature series of China back to 1873 and 1880, respectively. Tu (1984) has constructed a homogeneous temperature series for China, in which monthly

mean temperature observations of 42 stations in eastern China are used. The gaps are filled with the aid of interpolation. Wang et al. (1998b) constructed an annual mean temperature series of China from AD 1880 to 2002. It indicates that temperature has increased in general for the last 120 years period. The great increments occurred from the end of 1900's to the middle of 1940's, and from the middle of 1980's to the end of the series. The warming trend is  $0.58^{\circ}\text{C}/100\text{a}$  according to the series of 1880-2002.

For the reconstruction of climate in the last 20ka, the lake status data of CLSDB show that the climate at 6ka BP was wetter than today in north-eastern and northern China and most areas of western China. The lake records also suggest that southeastern China was drier than today. For 18ka BP ( $^{14}\text{C}$ ), lake status data show wetter conditions than that of today in western China (west of  $100^{\circ}\text{E}$ ) including the Tibetan Plateau and inland Xinjiang, but drier conditions in eastern China.

Quaternary climate records from South East Asia document large changes in environmental conditions during the Quaternary. The spatial pattern of these environmental changes provides insights into the changes in atmospheric circulation regimes that drive regional climates. The recognition of this fact has led to multiple attempts to synthesis and map the available palaeoenvironmental data from South East Asia (e.g. Winkler and Wang, 1993; Shi et al., 1993; Yu et al., 1998, 2000; Kohfeld and Harrison, 2003). These syntheses and interpretations are greatly supported by the existence of palaeoenvironmental databases (Kohfeld and Harrison, 2003), which provide comprehensive, well-documented and quality-controlled records from individual sites for continental-scale regions. There are three databases that provide such information for China: the Chinese Lake Status Database (CLSDB: Yu et al., 2001a, 2001b), the BIOME 6000 data sets for China (Yu et al., 1998, 2000), and the Chinese Loess database (Sun et al, 2000; Kohfeld and Harrison, 2003).

### 2.2.1 Loess

In the northwestern China, the loess plateau with maximum depth of 3000 m provides very important paleoclimate records (Ding *et al.*, 1994) for the million years before present. Temperatures and precipitation in the Quaternary (2.4~2.5Ma BP to present) are reconstructed based on the analyses of magnetization and the size of particles of loess. The reconstruction from loess records show that there were about thirty-seven glacial-interglacial cycles in the past 2.5Ma and with different periodicities. The 100ka periodicity appeared in the period from 700~0 ka BP, and the

period reduced to about 41ka from 0.7 to 1.6MaBP. The loess record also suggested that temperature during the Last Glacial Maximum (LGM) (21ka BP) was 6°~7°C lower than that of present, and precipitation was about 50% of the present normal.

The Chinese Loess Plateau contains an extensive record of aeolian deposition through multiple glacial–interglacial cycles. Independent chronologies based on pedostratigraphy, magnetic susceptibility, radiocarbon and luminescence dating have been developed for 79 sites from the Loess Plateau and the surrounding region and used to estimate aeolian mass accumulation rates (MARs) for marine isotope stage (MIS) 1 through 5 (Sun et al., 2000; Kohfeld and Harrison, 2003).

High resolution records of loess accumulation during the Holocene show that accumulation rates were relatively high initially and fell to a minimum between ca 7000 and 3000 a B.P. Harrison and Kohfeld (2003) have suggested that these low accumulation rates during the mid-Holocene reflect an expansion of the Pacific monsoon resulting in wetter conditions on the Loess Plateau. The timing of the onset and cessation of reduced dust accumulation varies from site to site, and probably reflects spatial patterning in the timing of increased monsoonal rainfall.

## 2.2.2 Ice cores

Ice cores are another useful proxy for understanding past climate changes. Ice cores provide several hundred years to ten thousands years long proxy climate records with a high time resolution. The typical ice cores, such as from Dunde and Guliya drillings in Tibetan Plateau are 130m and 300m, respectively. The analyses of particles numbers and the  $\delta^{18}\text{O}$  from Dunde ice core recorded the climate change during the last 40ka, especially for the Holocene. This record shows that the warmest period occurred from 3.6~2.6kaBP in the Holocene over Tibetan Plateau area. The unusual cold and dry event appeared at about 8.9~8.7kaBP, with temperature reduced 3.7k in 300a. Other typical climate periods, such as Little Ice Age (LIA), Medieval Warm Period (MWP) were also well determined from  $\delta^{18}\text{O}$  of ice core in Dunde. Comparison of  $\delta^{18}\text{O}$  from ice cores changes in Dunde and Greenland indicates significant stadial and interstadial alternations, and the evidence of abrupt climate change, such as the Younger Drays.

Guliya ice core provides longer climate records than that of Dunde. There are some ice cores from Dasuopu, Tanggula, Malan and other locations. Yao et al. compared  $\delta^{18}\text{O}$  records from four ice cores in Dasuopu (south), Guliya (west), Dunde (north) and Purogangri (centrl), respectively.

They reconstructed annual mean temperature series of Tibetan Plateau in the last 100a and found that climate in the Plateau is warming in the last 100a.

### **2.2.3 Tree rings (Dendroclimatology)**

The analyses of Qilian Mountain tree rings provide number of records for climate studies, which include winter and spring mean temperature in the last 1000a, tree ring width with 560a long, annual precipitation in the last 1100a, summer humidity index of 682a, Delingha 1000a precipitation, and precipitation in the 1437a in Zaidam . Tree rings collection from Tibetan Plateau include Dulan(1835a), Changdu (1000a), Wulan (824a). Besides these tree rings records, there are many records from Xinjiang, north-east China, and eastern China. Tree-ring data also provide information on precipitation variations in a relatively short time periods; one of the recent studies describe precipitation change in Qinghai for the last millennium (Shao *et al.*, 2004). Synthesis work of the tree-ring studies has provided decadal mean precipitation anomaly maps of western China from the 1600s to the 1990's (Wang *et al.*, 1991; Kang *et al.*, 1997, Wu *et al.*, 1981; Wu *et al.*, 1981; Yang *et al.*, 2002).

### **2.2.4 Historical documents**

Documentary data is one of the main proxy data in examining climate change in historical time. China has a long history and a plenty of historical document records. The historical documents most distributed in the eastern China, which including direct climate records about droughts, floods, rainfall, snow, freezing, frost, wind and fall dust. And also some of indirect records on climate are available, such as crop production, famine, population, insect diseases etc. Chinese historiographers and climatologists have done a lot work on the historical climate reconstruction for the last several thousand years, and set up the time series of climate changes in different regions. (Zhang Deer, 1981, 1997, Zhang Piyuan, 1996, Wang Shaowu, 1998b, Zheng Jingyun, 1993, Wu Xiangding *et al.*, 1981). Zhu Kezhen is the first Chinese scientist who studied climate change during the last 5000 years in China. He confirmed the warm and wet period in the middle Holocene, and three cold periods within the Little Ice Age were identified too (Zhu, 1972). In the middle of the 1970s, Chinese scientists started a project to study the droughts and floods for the last 500 years and

published the “Droughts/floods maps for the last 500 years in China” in 1981 (CMI, 1981). After that time the series of records of droughts and floods extended to over a 1000 years (Zhang *et al.*, 1997).

### 2.2.5 Stalagmite

In the present time current years, stalagmite as proxy data with high resolution is paid attention to and is used widely since it has a long time, accurate aging, and high resolution. Chinese scientists have been in the advance in the world due to their achievement on the paleoclimate studies by using stalagmite records. Their papers have been cited a lot. Tan Ming *et al.* (2003) disclosed the temperature variability in centennial scale and its spatial distribution by using integrated stalagmite and tree rings records. They found that the integrated climate record showed a temperature variation that is symmetrical like a “V” shape, not a “Hockey Stick” shape in the last 1000a in China. The minimum temperature was at “Spörer Minimum” and had the same pattern as climate in north Atlantic area. Therefore, this result confirmed that centennial variability of climate in eastern Asia and north Atlantic has the same phase in the last 1000a.

### 2.2.6 Pollen

Pollen data are widely used in the paleoclimate studies. From pollen analyses, many temperature anomaly series at different sites in China were reconstructed. The main shortcoming of the temperature anomaly series from pollen data is the low time resolution. Thus the pollen analysis is good for time averaged temperature in a period rather than for the single year or for high resolution study.

A typical case is the maximum temperature anomaly reconstruction of the Megathermal (mid-Holocene, ca 6ka BP, Shi, 1993). Temperature anomalies were also estimated according to the changes of vegetation (Zhang *et al.*, 1993).

China is one of the first regions to be considered in the BIOME 6000 project (Yu *et al.*, 1998) and there have been several subsequent attempts to improve the vegetation reconstructions (Yu *et al.*, 2000). Tests with a set of 840 modern pollen samples spanning all biomes and regions show convincing agreement between reconstructed biomes and present natural vegetation types, both geographically and in terms of the elevation gradients in mountain regions of northeastern and southwestern China.

### **2.2.7 Lake sediments**

Fluctuations in the water balance (precipitation minus evaporation: P-E) over the catchment of a lake are reflected in changes in lake area, level and volume, and can thus be reconstructed from geomorphic and stratigraphic records from the lake basin (Street-Perrott et al., 1989). Although such changes may be influenced by local non-climatic factors, regional-synchronous changes in lake area, level or volume (collectively referred to as lake status) are generally a response to climate. Thus, regional changes in lake status have been used to reconstruct regional palaeoclimates and the changes in atmospheric circulation patterns that gave rise to them (Harrison et al., 1996). Continental-scale reconstructions of changes in lake status have also been used as a benchmark to evaluate model simulations of changes in P-E (e.g. COHMAP, 1988; Qin et al., 1998).

The Global Lake Status Data Base (GLSDB: Qin et al., 1998) is an effort to compile the geomorphic and biostratigraphic data for changes in lake status for individual lake basins, in order to document changes in regional water balance during the last 40,000 years. The Chinese Lake Status Data Base (CLSDB: Yu et al., 2001a, 2001b) is a component of the GLSDB. Version 1 of the CLSDB contains 42 lakes (Yu et al., 2001a) and a further 26 lakes are included in an updated version of the data set (Yu et al., 2001b).

## **2.3 Climate simulation of the last 1000 years**

Historical climate simulation through long time integration is undergoing a rapid development phase. The numerical model simulation plays a vital role in understanding the causes and physical mechanisms of climate change on centennial time scale. In this section the temperature over the last millennium simulated by the global climate model ECHO-G is used to compare with the reconstructed temperature anomalies in the eastern China. The purposes are to test the skill of the model in simulating regional climate of China, and to understand the causes and mechanisms of the past climate changes in China (Liu et al., 2005). The present study may help improving our comprehensive understanding of the historical climate change, enhancing the forecast reliability for predicting the tendency of future climate change.



### 2.3.1 Model description

The climate model ECHO-G consists of the spectral atmospheric model ECHAM4 and the global ocean circulation model HOPE-G, both were implemented and developed at the Max-Planck-Institute of Meteorology (MPI) in Hamburg. ECHAM4 is a fourth generation of atmospheric general circulation model, which is based on primitive equations with a mixed p- $\sigma$  coordinate system. The horizontal resolution of the model is T30, or approximately  $3.75^{\circ} \times 3.75^{\circ}$ , and the vertical resolution is 19 levels with five upper levels being located above 200hpa. The horizontal resolution of the ocean model HOPE-G is about  $2.8^{\circ} \times 2.8^{\circ}$  with a grid refinement in the tropical regions, where the meridional grid point separation reaches  $0.5^{\circ}$ . The ocean model has 20 vertical levels. The model ECHO-G has been used in a number of simulations for the present and past climates.

Two 1000-year integrations with the ECHO-G model have been carried out at MPI. One is a control simulation, in which the external forcing is kept at constant values of the present climate. This experiment can simulate annual, inter annual and decadal climate oscillations that are determined by the internal dynamics of the coupled climate system, but cannot simulate the climate change caused by external forcing, such as the Medieval Warm Period and the Little Ice Age. Another experiment is externally forced simulation, in which the model ECHO-G was driven by three external forcing factors: solar variability, greenhouse gas concentrations in the atmosphere (including  $\text{CO}_2$  and  $\text{CH}_4$ ) and an estimation of radiative effects of stratospheric volcanic aerosols, for the period of 1000 to 1990 A.D. Further details of the simulations can be found in Storch et al. 2004. The result from the forced simulation is used for comparison with the reconstructed sequences in this section.

### 2.3.2 Reconstruction data

Abundant historical, documentary records on phonological events of cold/warm and dry/wet climate are available in China as described in last section. Numerous studies on reconstructing the historical climate change have been done by Chinese scientists using these documentary records. In recent years, Ge et al. conferred with and developed Zhu's method of deducing climate change for the past 5000 years using phonological records in China. They reconstructed winter half-year (October to April) temperature anomalies for the past 2000 years in the central region of eastern China ( $25^{\circ}$ – $40^{\circ}\text{N}$ , east of  $105^{\circ}\text{E}$ ) at 10–30 years resolutions. Their reconstructed temperature anomalies since 1000 A.D. at a 30-year resolution are

used here.

The study of climate change since Little Ice Age (LIA, 1550-1850AD) has been received extensive concern in China. Widely spread and severe famine and serious social turmoil have taken place in China during LIA (Xu, 1997). Because of this broad interest, the climate of China during the last 2000 years has been reconstructed by Chinese scientists, in particular temperature and precipitation since LIA with a variety of proxy data, such historical documents, tree rings, ice cores, lake warves, archaeological materials, etc. (Wang et al., 1998; Wang and Gong, 2000; Zheng and Zheng, 1993; Yao et al., 1996).

### **2.3.3 Model and data comparison**

The simulated temperature anomalies from the externally forced simulation with ECHO-G are first compared with 120-year observed data in eastern China ( $25^{\circ}$ – $40^{\circ}$ N, east of  $105^{\circ}$ E) in order to test the model's performance. Fig.2.1 compares the simulated and the observed variations of the winter-half year temperature anomalies in the eastern China since 1870. It can be seen that the increasing trends of temperature fluctuations in the eastern China are evident and consistent for both model output and observations. There is a statistically significant correlation between them at 99.5% confidence level, although the simulated mean temperature is about  $0.15^{\circ}\text{C}$  lower than the observed one. The uncertainty in Jones' observed data is of the same order, suggesting that the model results and Jones' data may be considerably consistent with each other.

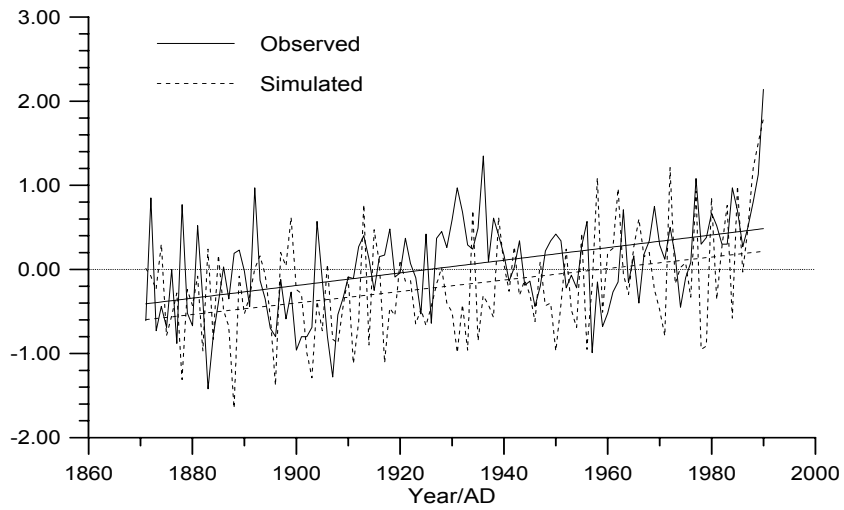
To be compatible in temporal resolution, we first compiled the winter-half year temperature anomalies in the eastern China ( $25^{\circ}$ – $40^{\circ}$ N,  $105^{\circ}$ – $123.75^{\circ}$ E, 20 grid points) from the externally forced simulation, and then calculated 30-year mean temperature anomalies. Finally, the simulated results are compared with reconstructed winter-half year temperature anomalies (at a 30-year resolution) of the eastern China. Figure 2.2 shows these two time series along with their corresponding polynomial fitting curves.

Figure 2.2 indicates that the reconstructed and the simulated results exhibit similar low-frequency variations and long-term trends. The range of the simulated temperature is from  $-0.70^{\circ}\text{C}$  to  $0.92^{\circ}\text{C}$ , and that of reconstructed is  $-1.1^{\circ}\text{C}$  to  $0.9^{\circ}\text{C}$ . The amplitude of the simulated temperature anomalies is about  $1.62^{\circ}\text{C}$ , slightly less than that of reconstructed ( $2.0^{\circ}\text{C}$ ). The correlation coefficient of the two time series is 0.37 that is significant

at 97.5% confidence level. Overall, both simulation and reconstruction show the Medieval Warm Period from 1000 to 1300, the Little Ice Age from 1300 to 1850, and the modern warming period since 1900. The anomalies from simulation and reconstruction in the Little Ice Age (1300–1850) and warming since 1900 are particularly consistent. Especially, both simulated and reconstructed temperatures reached their minimum values without phase difference during the Maunder Minimum of sunspots from 1670 to 1710. However, for the Medieval Warm Period of 1000–1300, the simulation and reconstruction show some phase differences: The reconstruction displays two peaks with one valley in between, whereas the simulation shows three peaks with two valleys in between.

It can be seen from Fig.2.1 that after 1500 the phases and amplitudes of the reconstruction and the simulation match better than those in the period prior to 1500 A. D. This may be related to the fact that less amount of data sites were used for climate reconstruction in the earlier period. Of also notable is that the difference between the simulation and reconstruction becomes large in the last 100 years. The simulation shows a faster increasing trend and higher than reconstructed temperature. The possible cause for this discrepancy may be partially due to the exclusion of the aerosol forcing in the forced experiment. The effects of aerosol have been thought to be a forcing factor that can offset the warming. It is conceivable that the regional cooling effect of aerosols could reduce the warming if they were included in the model, especially in the 20<sup>th</sup> century.

It is worthy to point out that the simulated temperature anomaly in the 20th century is higher than that in the Medieval Warm Period, while the reconstructed temperature in the 20th century is lower, albeit close to that of the Medieval Warm Period (Fig. 2.1). These two different results provide two different interpretations regarding the nature and amplitude of the recent global warming. One is that the 20th century warming has exceeded the normal range of the climate change, and it will result in catastrophic impact on human beings if warming continues going up. The other is that the current climate change has not yet exceeded the range of natural climate change in the past millennium. The final answer for this problem calls for both the improvement of the fidelity of the climate models in their long-term climate simulation and more profound work on quantitative reconstruction of paleo-climatological data. The latter requires reconstructing historical climate change sequences with higher resolution, precision, and reliability.



**Fig. 2.1** Comparison of model-simulated and the observed winter half-year temperature anomalies (Jones, 1998) in the eastern China. The anomalies are calculated with reference to the 1951–1980 mean temperature as shown by the dotted line.

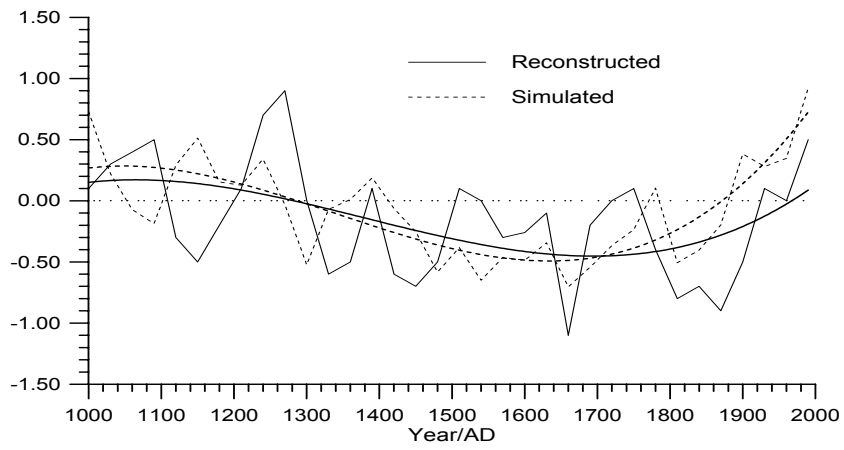


**Fig. 2.2** Comparison of simulated and reconstructed winter half-year temperature anomalies in the eastern China. Detailed explanation is referred to the text.

## 2.4 Sensitive simulation of climate in LIA

Promoted by the international research projects of PAGES and CLIVAR, the studies on climatic and environmental changes in the past 2000 years have drawn the attention of geologists and palaeoclimatologists all over the world. Among them the cold event of the Little Ice Age (LIA) is particularly the most attractive one, which is the nearest typical cold period in the global range from modern age, and had a profound impact upon human society. Additionally, more knowledge about the causes of origin and dynamic mechanisms of LIA may enrich and improve the theory of climatic changes on century scale, which can be used to predict the future tendency of climatic changes, and evaluate the possibility of cold vibrations on the global warming background.

There has been a half-century history of the LIA study abroad. Recently, based on the high-resolution and multi-environmental proxies from ice cores, tree rings, historical documents, lake sediments, corals and stalagmites, scientists have deeply known about the age, internal fluctuations and the characteristics of the climate and environment in LIA. Subsequently, setting out from the climatic control factors, the cause of LIA formation was effectively explained, by using the changes of those parameters, such as sequences of  $^{14}\text{C}$  in tree ring (related to solar activity), acidity of ice core (related to volcanic activity), and concentration of green house gases in ice core bubbles. Owing to the continual progresses in methods and techniques of climatic simulation, scientists have carried out the simulation experiments of LIA, and have made obvious progresses.

Studies on lots of historical documents, archaeological datum and kinds of climatic proxies (tree ring, ice core, lake sediment), Chinese scientists have worked hard and carefully on several aspects, including the main climatic characteristics and stages of LIA in China and the effect of LIA on Chinese social ecology and people's livelihood. The results mentioned above indicate an evident regional difference in origin, amplitude and duration of the change in temperature and precipitation. This part is about LIA simulations on the mechanisms of climatic changes during LIA by using a GCM (Liu et al., 2002).

### 2.4.1 Model description

A global model (AGCM + SSiB) is used which includes the terrestrial processes. The AGCM model is an improved nine-layer and fifteen-spectrum model, with horizontal resolution of  $7.5^\circ \times 4.5^\circ$ . The SSiB model is a simplified version of the simple biosphere model, in which

there is one vegetation layer with twelve vegetation types and three soil layers. After the calculation of SSiB, diagnostic variables are obtained, such as soil temperature and humidity in each layer, the temperature and moisture storage of the vegetation crown and ground temperature and snow amount, and SSiB and AGCM are coupled finally. Ever since the 1990s, Chinese climate modelers have made improvements in many aspects of the model.

### 2.4.2 Design of the simulation experiments

During LIA the solar radiation was 0.5% less than the average of modern time, the average optic depth of stratosphere volcanic dust is 0.15 and the vegetation of the underlain surface is slightly changed by human activities. We therefore design seven simulation experiments (Table 2.1).

In all the LIA simulation experiments (Table 2.1), atmospheric CO<sub>2</sub> level, sea surface temperature, background and preliminary field of atmospheric aerosol have consistent values. The integration time of the model is 15 years, taking the average result of the last 10 years as the equilibriums of these simulations. Running the experiments involved above, we can compare the effects and mechanisms caused by changes of solar radiation, optic depth of stratosphere volcanic dust, underlain surface vegetation and CO<sub>2</sub> content in the formation of LIA.

### 2.4.3 Analyses of simulation

#### *Temperature*

(1) Characteristics of the temperature change forced by a single factor. The differences between Exp.1 and Exp.2 reflect the possible effect of the decrease in solar radiation output by 0.5%, taking Exp.1 as the comparative standard experiment (control run). Fig. 2.3 shows the difference distribution of annual mean temperature, summer temperature and winter temperature in Eurasian continent between Exp.1 and Exp.2, respectively. The difference of annual mean temperature of the whole Eurasia is abnormally negative (Fig.2.3 (a)), except for the small region of Middle East and the Siberian high-latitude region. And the most remarkable temperature decrease appears in northeastern China and northern Africa, the mean maximum decrease may reach up to 0.6°C, mostly exceeding over 0.2°C. The summer temperature decrease is larger than that of winter. The whole Eurasia of the Eastern Hemisphere suffered from temperature decrease by over 0.2°C, the maximum is up to 1°C (Fig. 2.3 (b)). Compared with that

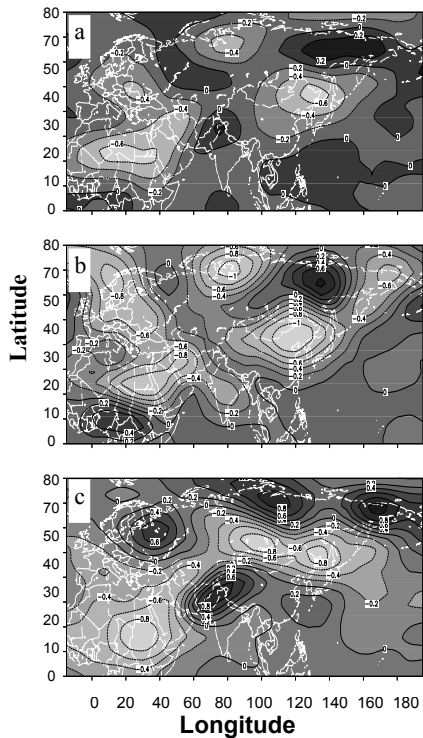
of summer, the temperature decrease of winter is smaller both in region and extent. Temperature still decreases in Northeastern China, whereas the increase occurs in the mid and west part of China. All the results above indicate that the reduced solar radiation, as the forcing mechanism of temperature decrease during LIA, has different effects on the seasonal temperature decrease; the temperature decrease is more evident in summer than in winter. Meanwhile, because of other feedback mechanisms, there is a large regional difference in the winter temperature change. However, the annual mean temperature decrease is the most obvious characteristic.

**Table 2.1** Characteristics of LIA simulation experiments

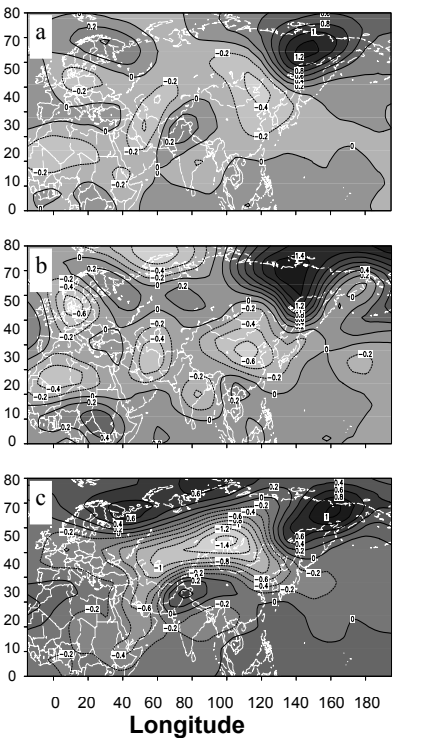
Expt.	Solar radiation ( $\text{w/m}^2$ )	Optic depth of volcanic dust	Type of underlain surface vegetation	CO <sub>2</sub> (ppm)	Remark
1	Modern value (1367.04)	Modern value	Modern	345	Control ex- periment
2	-0.5% (1360.165)	Modern value	Modern	345	Single-factor sensitivity experiment
3	Modern value (1367.04)	+0.15	Modern	345	Single-factor sensitivity experiment
4	Modern value (1367.04)	Modern value	Ante- Industrial- Revolution	345	Single-factor sensitivity experiment
5	-0.5% (1360.165)	+0.15	Modern	345	Double-factor sensitivity experiment
6	-0.5% (1360.165)	+0.15	Ante- Industrial- Revolution	345	Tri-factor sensitivity experiment
7	-0.5% (1360.165)	+0.15	Ante- Industrial- Revolution	280	Typical LIA experi- ment

Fig.2.4 gives the distribution of temperature difference between Exp.3 and Exp.1, which represents the temperature change effect after increasing the optic depth of stratospheric volcanic dust. The temperature decrease effected by volcanic dust is obvious, and the annual mean value is between 0~0.4°C, with the maximum of 0.4°C being in Northeastern China (Fig.2.4

(a). The temperature decrease is slightly smaller than that of Exp.2 in both region and extent. Compared with the figure about annual mean, summer mean, and winter mean change of temperature (Fig.2.4), the amplitudes of summer and winter mean change are apparently larger than that of annual mean. Additionally, the change in winter is more remarkable than in summer. The summer temperature decrease in most parts of China is between 0~0.6°C, while that is 0.2~0.8°C in winter, the maximum in the Siberian region is above 1.2°C. The results indicate that volcanic dust plays an important role in the winter temperature decrease. This decrease is opposite to the effect of temperature decrease caused by solar radiation. Moreover, comparing Fig.2.3 with Fig.2.4, the effect of temperature decrease arising from the change of volcanic dust is smaller than that from the reduction of solar radiation, however, their spatial distribution has some similarity.



**Fig. 2.3** The distribution of temperature difference between Exp.1 and Exp.2. (a) Annual mean; (b) summer mean; (c) winter mean.



**Fig. 2.4** The distribution of temperature difference between Exp.1 and Exp.3. (a) Annual mean; (b) summer mean; (c) winter mean.



(2) Characteristics of the temperature change forced by double factors. Fig.2.5 shows the temperature effect after reducing the solar radiation and increasing the optic depth of stratospheric volcanic dust. In these maps, annual mean temperature in Eurasia still decreases. The annual mean temperature decrease in China is between  $0.2\sim 0.4^{\circ}\text{C}$ , and that in Europe and most parts of North Africa is above  $0.2^{\circ}\text{C}$  (Fig.2.5 (a)). Comparing with Fig.2.3(a) and Fig.2.4(a), the region of maximum temperature decrease above  $0.4^{\circ}\text{C}$  in Fig.2.5 (a) extends, which reflects that the synchronous function caused by the reduction of solar radiation and the increase of optic depth of volcanic dust has a superposed strengthening effect on the temperature decrease in large regions. The main regions of summer temperature decrease include the whole Eurasia, especially in East China, whose central part is North China, with an amplitude of  $0.2\sim 1.0^{\circ}\text{C}$ . The range of summer temperature decrease is still larger than that of the annual average. In winter the center of temperature decrease in Eurasia moves to the west, the center of maximum temperature decrease approximately above  $1^{\circ}\text{C}$ . And the east part of China turns into an uneven decrease region. The most remarkable temperature decrease occurs in North East and South China, while the slight temperature increase appears in West China.

In the analysis of the results of simulation experiments mentioned above, both the reduction of solar radiation and the increase of the optic depth of stratospheric volcanic dust can result in the air temperature decrease of land surface, but because the mechanism of decrease in temperature and the background of atmospheric circulation are different, the extent of the decrease and the regional distribution are not the same. However, the integrated effect is to decrease the temperature, to make the distribution more even, and to strengthen the average extent of temperature decrease.

(3) Temperature effect resulting from the change of vegetation and  $\text{CO}_2$  concentration is another important topic in the LIA climate change. Many research and simulation experiments indicate that the change of vegetation plays an important role in the air temperature of land surface in the certain time scale and climatic background. When performing the LIA climate simulation experiments, two types of vegetation are chosen for making comparison, modern vegetation and vegetation before Industrial Revolution. As a whole, the latter has a larger rate of natural vegetation coverage than that of the former. The result of Exp.4 indicates that the change of vegetation field engenders different tendency in temperature change, i.e. the annual mean temperature increased in East Asia, while that of North Africa decreased significantly (figure omitted). Thus the promotion of the vegetation coverage profits the increase of temperature, and the decrease of vegetation coverage contributes to the decrease in temperature of the land surface. Because the LIA climate turned cold, the vegetation coverage

in some regions of China became smaller. So, from this point of view the vegetation status has played a certain role in the formation of LIA climate. For lack of the more completed vegetation status in LIA, the simulation experiments with real vegetation coverage in LIA did not perform.

### **Precipitation**

(1) Precipitation effect caused by the reduction of solar radiation is shown in Fig.2.6 and Fig. 2.7. Fig.2.7(a) shows the difference of precipitation distribution between Exp.2 and Exp.1. It can be seen that there is no evident change of annual precipitation in the whole Eurasia, while precipitation increases significantly in the West Pacific Region. The increase in annual precipitation in the West Pacific Region and the South East China is above 0.3 mm/d, and that in North West and Mid of China is about 0~0.3 mm/d, approximately 100 mm/a or so. Precipitation in other regions slightly decreases or remains as usual. While in summer the precipitation changes evidently, increasing in East Asia, South Asia and Indian region. In the most parts of China, except the littoral region in South China, the precipitation variation is positive abnormally, especially in east part of China, with an increase about 0.5~1.0 mm/d, which amounts to 50~100 mm in the three months of summer. Meanwhile, precipitation also increases in the equator TCZ, South Asia, Northwestern Pacific Ocean and Indian Ocean, but decreases in the South China Sea and Bengal Bay. The change of winter precipitation is similar to that of the annual precipitation. Except the South China Sea and the West Pacific Ocean with an increase of 0.5~1.5 mm/d, there is nearly no change in the mainland of China. These characteristics of precipitation uncover that summer monsoon circulation and precipitation change in East Asia with the change of solar radiation, that is, certain decrease in insolation will profit increase in precipitation of summer monsoon in East Asia.

(2) Precipitation change caused by effect of volcanic dust is shown in Fig.2.7. Fig.2.7 (a) indicates that the increase in the optic depth of volcanic dust does not affect the annual precipitation in most parts of the Eurasian continent, while precipitation increases slightly in the region of China and India in East Asia. Furthermore, there is still a significant increase in precipitation in the region of the Western Pacific Ocean. The change of annual precipitation is less than 50 mm, or even unchanged in most parts of China. Meanwhile, precipitation changes insignificantly in the region near the equator. This tendency is strengthened in summer, and precipitation increases evidently in the middle of China. The increase range in the Indian subcontinent is approximate to that in the region of East Asia. In China from southeast littoral to inland, the increase range is between 0~1 mm/d,

which means that the maximum change in summer precipitation can reach about 50~100 mm. The significant decrease in precipitation still occurs in the South China Sea. There is an evident increase in precipitation in the Western Pacific Ocean and equator TCZ, with the maximum value of 2.5 mm/d. This phenomenon probably implies that the increase in the optic depth of volcanic dust can intensify the precipitation caused by Southwestern Monsoon and South western Air current, while in other non-monsoon regions the effect of volcanic dust is not significant (Fig.2.7 (b)). The fact that the winter precipitation decreases in South Asia and slightly increases in Mid-Asia may indicate its relationship with the activity of southern branch of westerly (Fig.2.7(c)).

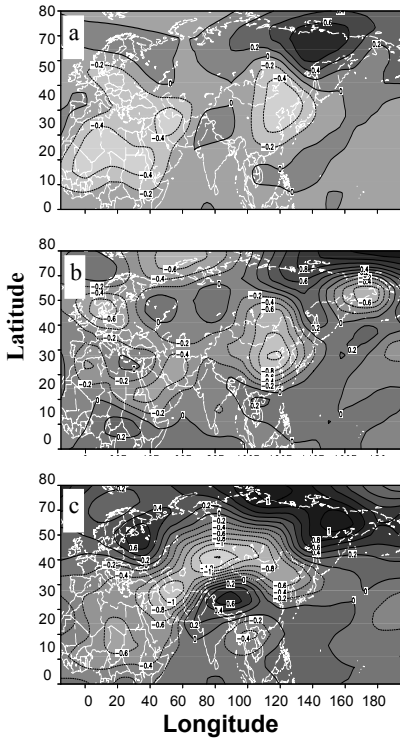


**Fig. 2.5.** The distribution of temperature difference between Exp.1 and Exp.5. (a) Annual mean; (b) summer mean; (c) winter mean.

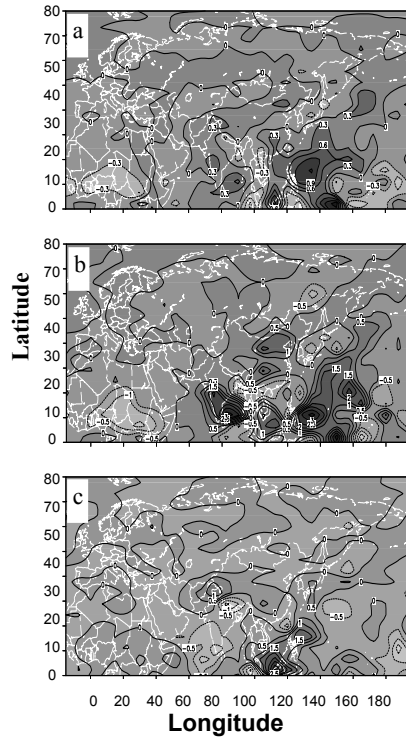


**Fig. 2.6.** The distribution of precipitation difference between Exp.1 and Exp.2. (a) Annual mean; (b) summer mean; (c) winter mean.

(3) Precipitation change affected by double factors. Fig.2.8 shows the precipitation change caused by both the reduction of insolation and the increase in the optic depth of stratosphere volcanic dust. The composite effects of the two forcing factors cause the increase in annual precipitation in East Asia, especially in East China. The maximum of that is 0.3 mm/d, equal to about 100 mm/a, while the decreases in annual precipitation in both Southeast Asian and Indian region. The spatial distribution pattern of summer precipitation is similar to that of annual precipitation, but the ranges of increase and decrease become larger; and the summer precipitation increases by above 0.5 mm/d (approximately 46 mm in the season) in East China; the maximum is more than 90 mm, while the summer precipitation decreases by above 1 mm/d (90 mm) in South Asia; the maximum exceeds 180 mm. The winter precipitation does not change evidently in the whole Eurasia, but there is a maximum center in Mid-Asia where the precipitation increases over 40 mm. The conclusion is that the composite effects of both factors are to promote the precipitation of summer monsoon in East China, and to reduce the southwestern monsoon precipitation in South Asia.

Precipitation change affected by the change of vegetation. After changing the status of vegetation (Exp.4), the annual precipitation increases significantly in East Asia, and the precipitation of summer monsoon also increases by 46~160 mm. Meanwhile, there is evident precipitation increase in India and Southeast Asia, while precipitation decreases in Mid-Africa. Winter precipitation does not change significantly. It is suggested from these analyses that, after coupling with vegetation component, precipitation increases where the vegetation coverage increased (e.g. East Asia); when the vegetation coverage reduces (e.g. North Africa), the precipitation decreases, too.

## 2.5 Palaeoclimate simulations of mid-Holocene and LGM

Reconstructions from proxy data, including pollen, lake-level, and loess records, have been providing a picture of regional climate changes of China during the Quaternary. The General Circulation Models (GCMs) has been used to explore the mechanisms of observed regional and global climate in the past decades. By use of GCMs, we can simulate the atmospheric response to the external forcing in LGM (21ka B.P.) and mid-Holocene (6ka B.P.). Some model simulations have demonstrated the importance of land-surface and ocean feedbacks for regional climates. Here we introduce the results of equilibrium climate simulation for the East Asia

by using prescribed vegetation coverage corresponding to the observed changes in vegetation patterns for these two periods. Comparisons of model simulations with palaeoclimate data from China show how far we can explain past climate changes and the confidence that can be placed in current state-of-the-art models.

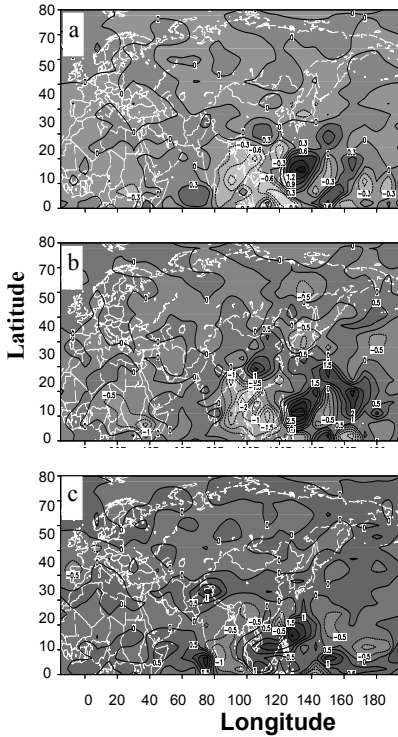


**Fig. 2.7.** The distribution of precipitation difference between Exp.1 and Exp.3. (a) Annual mean; (b) summer mean; (c) winter mean.

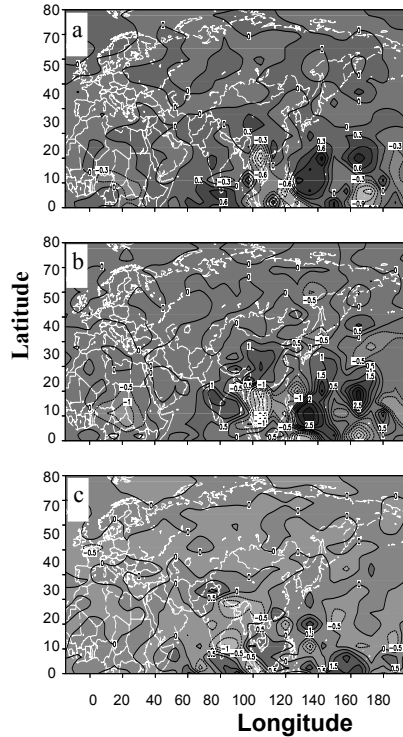


**Fig. 2.8** The distribution of precipitation difference between Exp.1 and Exp.5. (a) Annual mean; (b) summer mean; (c) winter mean.

As we known that the Palaeoclimate Modelling Intercomparison Project (PMIP: Joussaume and Taylor, 1995; Joussaume and Taylor, 1999) has examined how the northern hemisphere monsoons responded to changes in climatic forcing at the last glacial maximum (LGM, ca 21 ka BP. equivalent to ca 18  $^{14}\text{C}$  ka BP.) and during the mid-Holocene (Pinot et al., 1996; Joussaume et al., 1999). These two intervals represent two climate extremes.

The model used here is the same as that used in LIA simulation, AGCM+SSiB to simulate climate changes in the Asian region at 6 ka BP and 21 ka BP. The experimental design for the 6 ka BP and 21 ka BP. experiments followed the PMIP protocol (Joussaume and Taylor, 1995) and some changes are made according to the reconstructed vegetation data in order to investigate the importance of vegetation feedbacks on regional climates over Asia.

The BIOME 6000 vegetation data sets for 6 ka BP and 21 ka BP. (Version 4.0: Prentice et al., 1996; Yu et al., 1998; Yu et al., 2000) were used as the basis for the derived land-surface characteristics. The pollen-based reconstructions at each site in the BIOME 6000 data set were interpolated to the grid of the climate model; grid cells containing multiple pollen sites were attributed to the modal vegetation type, and no change was made to grid cells lacking pollen sites.

### **2.5.1 The 6 ka BP climate simulations**

It is important for us to understand a similar impact of climate warming in response to the increased atmospheric carbon dioxide in the future, and climate warming in response to one likely consequence of the changes in radiation forcing in the mid-Holocene (6 kaBP), which has become one of hot topics in international community of Global Changes.

An international project for paleoclimate modeling at 6 kaBP (PMIP: Paleoclimate Modeling Intercomparison Project) was launched in 1990s and has made great progresses. However, some important issues have not resolved so far. The PMIP designed a program for AGCM (Atmospheric General Circulation Model) simulations in which variations of solar radiation is considered as a major dynamic force for 6 kaBP climate. As the solar radiation variation played a unique role in the simulations, consequently most of the AGCMs have simulated the paleoclimate of 6ka BP with a general pattern of a warm summer and a cold winter over the major continents of the world.

However, synthesized studies from Quaternary data indicate that winter temperature at 6 kaBP was 2.5°C warmer in the east and 3-4°C warmer in the west of China than that at the present. This warm climate condition was recorded not only in China, but also in northern America. These facts do not agree with the modeling results that were only driven by solar radiation. Therefore, there would be other control factors that contributed to the warm climate at 6 ka BP, especially to the winter warming. It is necessary

for us to explore the causes of winter warming in the mid-Holocene in the East Asia.

Studies from TEMPO Program have revealed that, after introducing the feedback of surface albedo with a coupled climate-biome model, a northward-shift climate zone in northern Africa can be simulated. Chinese scientists also did modeling experiments to test the impact of vegetation on the monsoon precipitation. Claussen et al., (1996) found that the influence of changed orbital geometry of the Earth has been amplified in the climate change in subtropical climate zone because of the feedback of atmosphere and vegetation. It is likely believed that changes in the regional and global vegetation have strong feedbacks on climates of the mid-Holocene.

Although the above studies have suggested that the climate at 6kaBP was directly or indirectly controlled by a feedback between climate and land surface, the simulations of PMIP before 1999 did not include the forcing from an active land surface in the boundary conditions of the modeling experiments. This caused that modeling results disagreed with observed data from the East Asia, especially they produced a contrary result for winter temperature in China.

In this section, an AGCM plus SSiB was used to simulate climate at 6 ka BP. As an improved dynamical factor, land surface conditions of vegetation at 6 ka BP were reconstructed from geological records and input into the climate model in order to simulate more realistic features of paleoclimate (Chen et al., 2002).

### ***Forcing conditions***

Forcing conditions for control test (0 kaBP) are based on modern climate, including orbital geometry of the earth (1950 AD), atmospheric CO<sub>2</sub> concentration (345ppm), sea surface temperature (SST), vegetation distribution, and ice or snow coverage.

The paleoclimate simulation is designed in two experiments. The forcing conditions for Experiment One of 6 kaBP climate (Exp. 1) are prescribed according to a standard prescription from the PMIP. The orbital geometry of the Earth is from Berger's studies. CO<sub>2</sub> is set to 280 ppm. SST, vegetation, and ice or snow coverage are prescribed as the present-day conditions. In Experiment Two of 6 kaBP climate (Exp. 2), solar radiation, SST, ice or snow coverage and CO<sub>2</sub> are the same as Exp. 1, but we used paleovegetation at 6 ka BP instead of a prescribed one from modern vegetation. The vegetation distribution at 6 kaBP is reconstructed from pollen data over major continents by using biomization method. This method is good at translating pollen data into vegetation types. Yu (1998) introduced

how to translate pollen data of 6 kaBP into vegetation types in detail. We interpolated the point-type vegetation data into grid data by  $4.5^{\circ} \times 7.5^{\circ}$  grids in order to match the resolution of the AGCM. Forcing conditions of control test (0 kaBP) and 6 kaBP simulations are listed in Table 2.2.

Table 2.2 Forcing conditions used in the simulation experiments

Forcing condition		0 kaBP	6 kaBP
Orbital parameter (Berger)	Obliquity	23.446	24.105
	Eccentricity	0.016724	0.018682
	Perihelion	282.04	180.87
Topography		present	Same as 0 kaBP
SST		present	Same as 0 kaBP
Sea ice		present	Same as 0 kaBP
Ice sheet		present	Same as 0 kaBP
CO <sub>2</sub> concentration		345 ppm	280 ppm
Vegetation		present	Based on pollen data

**Results and Analysis of the Simulations at 6 kaBP**

11-year model run was made under the forcing conditions for 6 kaBP simulations. The average of the last 10 years was treated as mean climate condition.

**Temperature simulation in Exp. 1**

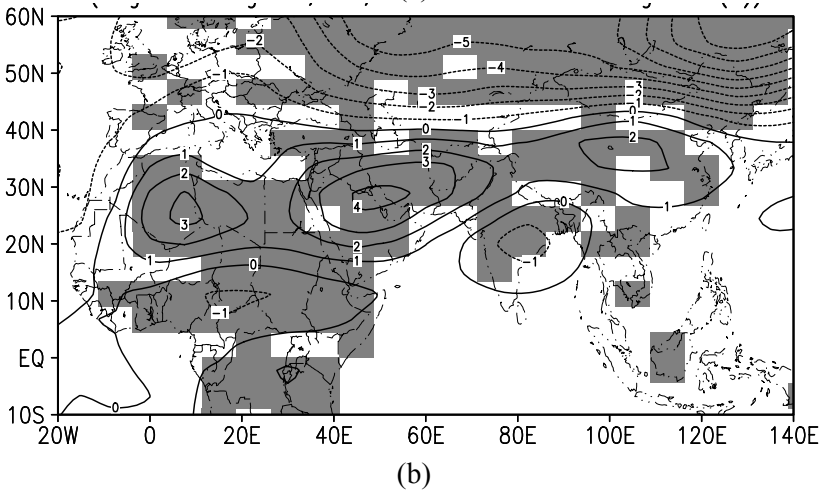
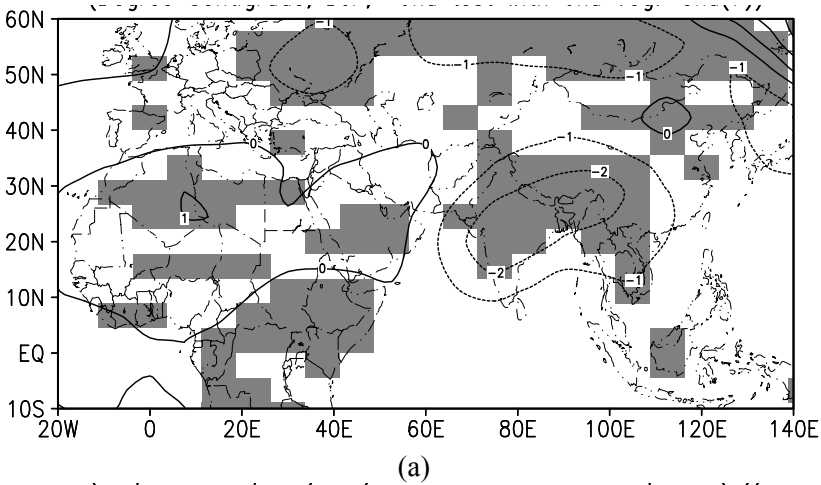
Fig.2.9 plotted the differences of simulated temperature between 6 kaBP and 0 kaBP. In the west of Eurasia, annual temperature at 6 kaBP was 0-0.5°C warmer than that in the present in the south of 50°N, and colder than present in the north of 50°N (Fig.2.9a). In the East Asia, summer temperature was about 2.0°C warmer at 6 kaBP than the present in the south of 40°N (Fig.2.9b), and winter temperature decreased about 2.0°C (Fig.2.9c) at 6 kaBP comparing with the present. This result agrees with those of PMIP climate simulations at 6ka BP.

PMIP standard simulations at 6 kaBP revealed a typical Post-glacial climate when Quaternary ice sheets were melted in the Northern Hemisphere. In views of climate dynamical mechanisms, solar radiation is the fundamental basic forcing that causes changes in climate warming globally and extensions of African and Indian monsoons regionally. Similar to all of the PMIP simulations at 6 kaBP, the Exp. 1 also showed annual and summer temperature about 1°C increases and significant decrease in winter



temperature in the low and middle latitudes (20-50°N) of Eurasian continent.

During the Holocene, the summer solar radiation reached the maximum at 9 kaBP (11 kaBP in calendar year) in the Northern Hemisphere, and was 7-8% greater in summer and 2-3% less in winter than present in middle and low latitude area (south of 50°N). This abnormal pattern had continued to the mid-Holocene (6 kaBP) and becomes a key reason why the PMIP climate simulations and the Exp. 1 modeled the cold temperatures in winter at 6 kaBP.



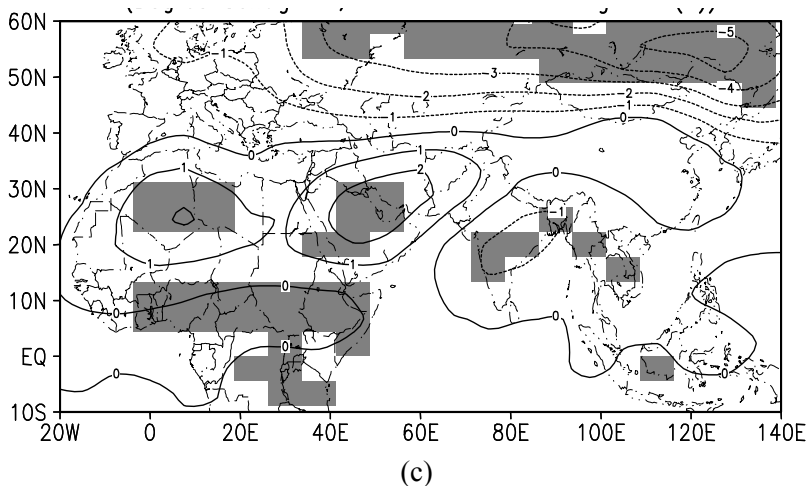


**Fig. 2.9** Differences of simulated temperatures between 6ka BP (Exp. 1) and 0ka BP, (a) Difference of annual temperature ( $^{\circ}\text{C}$ ), (b) Difference of summer temperature ( $^{\circ}\text{C}$ ), (c) Difference of winter temperature ( $^{\circ}\text{C}$ )

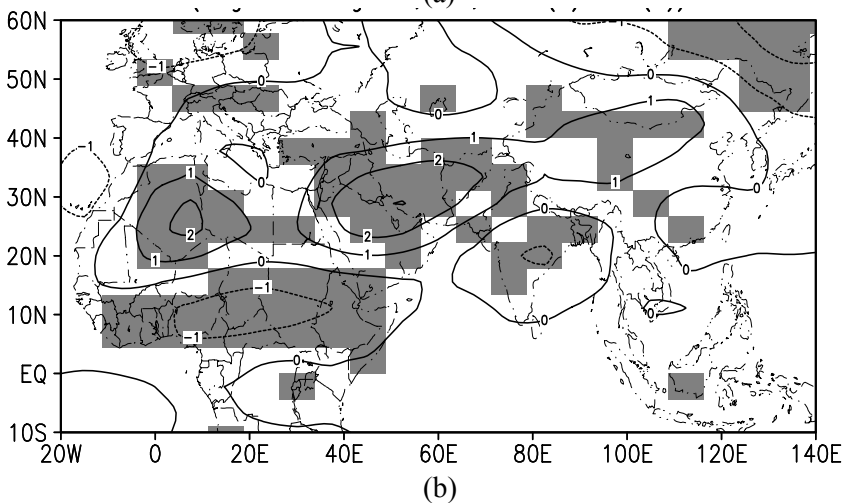
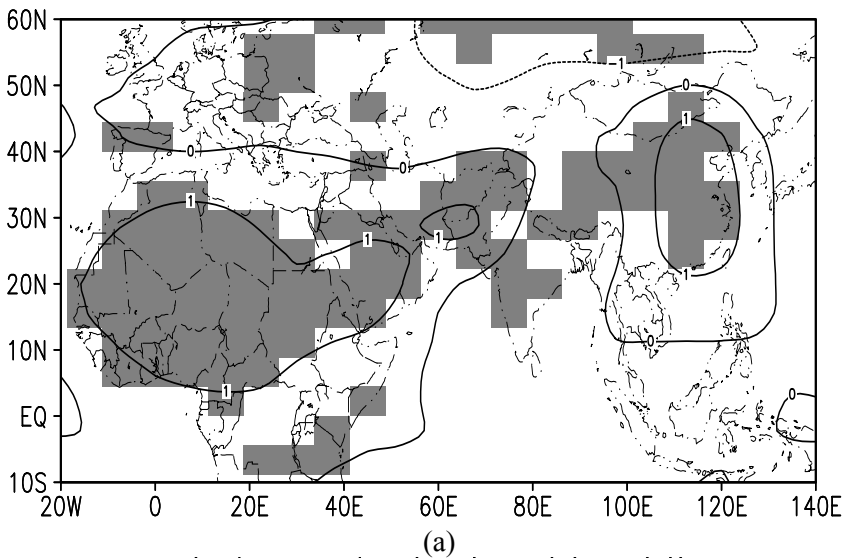
### Temperature simulation in Exp. 2

In the Exp.2, the vegetation distribution at 6 kaBP is used as land surface coverage in the modeling. The differences of temperature between Exp. 2 and control test (Figs not given) in the East Asia indicate ca 1-2 $^{\circ}\text{C}$  warmer in summer and ca 0.5-1.0 $^{\circ}\text{C}$  warmer in winter at 6 kaBP than the present. The annual temperature at 6 kaBP increased about 0.5-1.5 $^{\circ}\text{C}$  over all of the East Asia. The results imply that Exp. 2 has much more improvement in temperature simulation of 6 kaBP than Exp. 1. To compare the temperature simulations between the two experiments, we computed the temperature differences between Exp. 2 and Exp. 1 in order to understand the net effect of the vegetation on the temperature changes (Fig.2.10a, b and c). The index was shown in Fig. 2.10.

Simulated annual temperature in Exp. 2 was higher than that in Exp. 1 in the north of 50 $^{\circ}\text{N}$  in Europe, but it was slightly lower in Exp. 2 than Exp. 1 in Siberian area. In the south of 50 $^{\circ}\text{N}$ , annual temperature was about 1-2 $^{\circ}\text{C}$  higher than that in Exp. 1 in the eastern and northern China. There was no significant change of summer temperature between Exps. 1 and 2 (Fig.2.10b). However, winter temperature in Exp. 2 was 1 $^{\circ}\text{C}$  higher than Exp. 1 in the middle and eastern parts of China in the south of 50 $^{\circ}\text{N}$  (Fig. 2.10c)

Exp. 2 did not show a significant temperature change in Tibetan Plateau at 6 kaBP. It was 1-2 $^{\circ}\text{C}$  lower in winter in the central Plateau and 1 $^{\circ}\text{C}$

warmer in summer of north plateau than those in Exp. 1. Modern summer warming in the plateau is mainly due to increased solar radiation, which the summer heating is a major contribution to the annual temperature increase due to the specific geographical position and atmospheric optical characteristics of the plateau. Thus the warming effects should not mainly come from the vegetation changes in the plateau region. However, it is necessary to further study the causes of temperature change in the plateau in terms of the specific horizontal and vertical structures, the independent pressure system, and the planetary westerly over the Tibetan Plateau, e.g. using coupled climate-vegetation model to explore the possible mechanisms of climate at 6 kaBP.



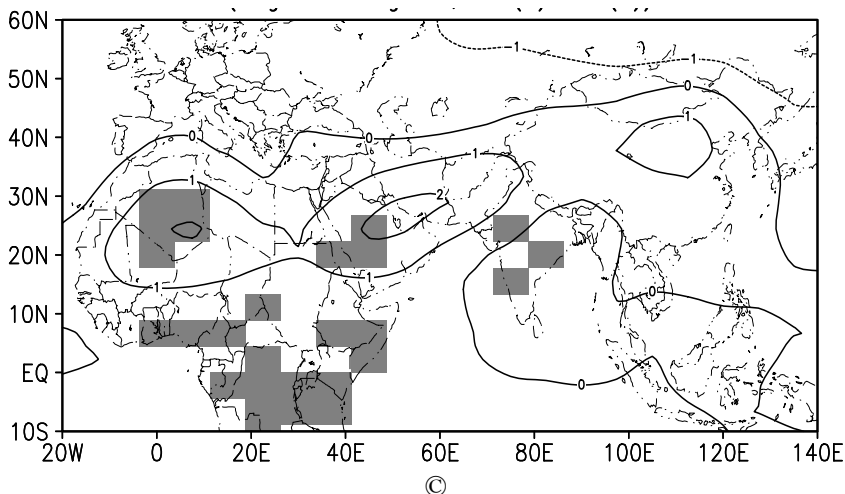


**Fig. 2.10** Differences of simulated temperature at 6 kaBP between Exp. 2 and Exp.1, (a) Difference of annual temperature ( $^{\circ}\text{C}$ ), (b) Difference of summer temperature ( $^{\circ}\text{C}$ ), (c) Difference of winter temperature ( $^{\circ}\text{C}$ )

### Significant test of simulations

From above analysis we can see that changes of solar radiation and vegetation in the mid-Holocene (6 kaBP) have played very important roles in the climate changes. Here we give the results of significant test for these simulation changes. By using T-student test at 95% confidence limit, two pairs of experiments (0 ka BP and 6 ka BP in Exp. 1, 6ka BP in Exp. 1 and 6 ka BP in Exp. 2) have been performed by T-test processes. Significant areas for each pair of parameters are shadowed in Fig.2.9 and Fig.2.10. In Exp. 1, when solar radiation is considered as a unique forcing factor, both summer warming and winter cooling in the East Asia are significant. The simulation of winter temperature by vegetation forcing in Exp. 2 has the largest significant areas in the east parts of China, and also larger significant area in the subtropics area (western Asia and northern Africa). Significant test showed that increases in annual and summer precipitation are significant in the middle latitude of the East Asia ( $30^{\circ}\text{N}$ – $50^{\circ}\text{N}$ ), northern Africa, and western China (Figs not shown).

### Data and model comparison of climate at 6 ka BP

Paleoclimate records can provide a reconstructed climate in the mid-Holocene in China, on basis of studies in Quaternary sciences, paleoclimatology and paleoenvironmental sciences. Records from pollen, fossil plants

and animals, paleosoils, lakes, ice cores, and the Neolithic archaeological evidences have reconstructed that annual mean temperature was higher than the present in China in the mid-Holocene. Researchers used various proxy indices to reconstruct qualitatively climate change (such as warm and wet, hot and dry, cool and mild, etc.) and to transform quantitatively temperature estimates. Pollen data indicate that paleovegetation belts shifted northward in latitude and upward in altitude. Records of macrofossils of animals and plants have estimated temperature of the mid-Holocene on basis of animal groups immigrated northward to a large extent. The paleosoils development and anthropological traces (traces of ancient human) in loess series, the change of oxygen isotope in ice core, historical documents and archaeological evidence of animal distributions all indicated a warm condition in the mid-Holocene. Based on these studies we estimated quantitatively mean temperature of annual, summer, and winter at 6 kaBP.

The annual mean temperature (from 43 sites), summer temperature (from 7 sites), and winter temperature (from 12 sites) are presented by differences of temperature between 6kaBP and 0ka BP in each geological site. In climatological studies, summer temperature infers to the mean temperature of June, July and August. In the geological studies, the definition of summer temperature is not accurate since some people used three months of June, July and August, but others may use the warmest month (July), so did the definitions in winter. Here, we included both climatological and geological definitions as semi-quantitative climate parameters. Result shows that annual mean temperature at 6 kaBP was about 1-5°C higher in the western China and about 3-4°C higher in the North China than the present. Exp. 1 has simulated about 0.5°C warmer in this area, but Exp. 2 showed 1-2°C warmer, suggesting that Exp. 2 has made great improvement comparing with the geological data. The winter temperature at 6 kaBP was about 3°C higher than the present in China. Exp. 2 simulated about 1-2°C higher in winter in this region, which agreed with extents of temperature changes from estimate of geological data. Summer temperature change at 6 ka BP was smaller than winter, about 1-2°C. The Exps. 1 and 2 have simulated similar summer temperatures to the geological data.

Improved surface condition in Exp. 2 has produced a better climate simulation with increased winter temperature at 6 kaBP. This simulation revealed the potential effects of both solar radiation and vegetation on the climate change, because the simulated winter warming is very much approaching to the reconstructed climate from geological data at 6 kaBP. Our climate simulation of 6 kaBP has also improved PMIP simulation of 6 kaBP. It should be pointed out that the pollen data could respond to the mean status of annual temperature and the plants growing season in spring-

summer. To improve the comparisons, more proxy data and the analyses are necessary.

### ***Mechanisms of vegetation effects on climate change***

The simulations suggested that increased solar radiation in the mid-Holocene played a major role in global warming, and increases in regional precipitation were mainly controlled by feedback of vegetation forcing. Foley et al., (1994) pointed out that the main cause of 6 kaBP warming in the high latitudes (60-90°N) of North Hemisphere is due to the decrease in the surface albedo because forests were extending northward and replacing tundra. Claussen et al (1999) discussed the sensitivities of vegetation and climate change over northern Africa in the mid-Holocene, suggesting that the regions with more vegetation coverage could not only absorb more solar radiation on the surface, but also increase surface evaporation, which could enhance greenhouse effect and lead to warm and wet climate comparing with bare surface conditions. TEMPO members (1996) found that the position of the northern border of forests in the mid-Holocene was related with temperature increases, especially the changes in vegetation could caused warming in summer (July), ca. 1.5°C to 4.0°C higher than that in 0 kaBP. Bonan et al., (1992) suggested that winter and summer temperature in the high latitudes (60-90°N) would increase when forests replaced tundra because of significantly reduced surface albedo. Studies of paleovegetation in the mid-Holocene showed that in the east part of China (east of 100°E), tropical broadleaf-evergreen trees extended northward and the large area covered by forests that replaced groundcover and desert in Inner Mongolia. At the same time, forests in Tibetan Plateau were extended upward at the high altitude. Therefore, the change and extension of vegetation coverage in large-scale would result in the spatial variation of the earth surface albedos. According to the vegetation distribution used in present simulation, needle leaved evergreen trees in mid-Holocene extended to the areas of modern tundra in the north part of Eurasia continent. Modern deciduous needle leaved trees forest in the high latitude of eastern Eurasia area was covered by needle leaved evergreen forest in the mid-Holocene. There were broad-leaf-evergreen trees that shifted northward in the east part of China. Broad-leaf trees and groundcover in northern Africa in subtropical latitudes covered deserts in the mid-Holocene. These evidences suggested: (1) When deciduous-trees was replaced by evergreen trees, the surface albedo in winter was reduced from 0.14 to 0.12 and annual average surface albedo kept same values 0.12 as today. (2) When desert and bare soil were replaced by groundcover, surface albedo decreased either. (3) When tundra in high latitudes replaced by coniferous-evergreen trees, the average sur-

face albedo changed from 0.16-0.17 to 0.10-0.12. Because of decrease in surface albedo, especially the winter albedo, it can create a warmer effect on climate in the mid-Holocene. Decreases in winter surface albedo, as a consequence of vegetation changes in the south part of China, would be equivalent to increases in surface net radiation and lead to increase in winter temperature.

According to the heat balance on the earth surface, changes in the surface albedo would lead to the differences of the thermal contrast between land and ocean, and lead to variations of monsoon circulation in the Eastern Asia. From the seasonal sea level pressure differences between Exp. 1 and Exp. 2 (Figs. Not shown), there is an enhanced low-pressure system over the East Asia and a subtropical high-pressure over Northwestern Pacific Ocean in the summer. As a result, difference between land and ocean would cause a strong summer monsoon circulation. In winter, high-pressure system over the East Asian continent and pressure system over northwest Pacific all became weaker in the mid-Holocene. The possible cause of this monsoon circulation change is likely that the tundra in high latitude area retreated to polar area, and coniferous leaved trees extended northward in a large-scale. Changes in the surface vegetation cover in the high latitude would increase earth surface thermo capacity, reduced cooling in high latitude, and weaken the cold high-pressure system over the continent. Thus, weakened winter monsoon circulation in the Eastern Asia would reduce the winter cooling, although there was an cooling effect of solar radiation decrease in the middle and low latitude areas (0-40°N). Furthermore, variation of the earth surface albedo from vegetation change in the mid-Holocene led to differences of seasonal thermo contrast between land surface of the East Asia and sea surface of northwest Pacific Ocean. As a result, summer monsoon circulation in the mid-Holocene became stronger than the present and wetter climate is formed.

## **Discussion**

Based on two sets of boundary conditions, i.e. PMIP setting at 6 kaBP (Exp. 1) and paleovegetation setting (Expt. 2), the climate at 6 kaBP was simulated by using AGCM+SsiB. Exp. 1 simulated about 1-2°C increase in annual mean temperature and about 2°C decrease in high latitudes in the East Asia. Exp. 1 revealed solar radiation driving and responded to the change of orbital geometry of the Earth in the mid-Holocene. This result is similar to those of most PMIP climate simulations at 6 kaBP in the late of 1990s.

Simulation of Exp. 2 explored the warming effects of vegetation under solar radiation forcing in the mid-Holocene. Annual mean temperature was

about 1-2°C warmer and winter temperature was 2-4°C warmer in the Eastern Asia. This fact revealed the vegetation effects on the climate warming through reducing surface albedo. Even though there are some discrepancies with geological records, results of Exp. 2 made a great improvement for winter temperature simulation in the mid-Holocene, suggesting that surface vegetation plays a very important role in changes of the seasonal and regional climate at 6 kaBP.

The comparison of simulation experiments shows that surface albedo variation due to vegetation change can produce the seasonal change in the thermodynamic differences between land surface in the Eastern Asia and sea surface over western Pacific Ocean in the mid-Holocene. On the other hand, forest extending in high latitude regions has increased the thermal capacity on the surface and reduced the cooling effects. As a result, the winter monsoon circulation was weakened and cold air activity was limited, leading to the winter temperature increased. Next work will need, in paleoclimate modeling, especially developing simulation experiments with coupled climate-biome models to improve simulation so that we can fully understand the physical processes and mechanisms of the paleoclimate change.

### **2.5.2 The 21 ka BP climate simulations**

Last Glacial Maximum (21ka BP) is another hot topic in the field of paleoclimate study. Recently, a lot of research results from data analysis of palaeoclimate and numerical simulation reveal that global climate at 21ka is very different from that in the present due to the existence of north-hemispheric icesheets, low concentration of CO<sub>2</sub>, different sea surface temperatures (SSTs), and orbital-forcing insolation anomalies (CLIMAP Members, 1981; COHMAP Members, 1988; Harrison et al., 1996; Kotlia et al., 1997; Street-Perrott et al., 1989; Tarasov et al., 1994; Wright et al., 1993). Quaternary researches in China reveal very different climate patterns at 21ka BP comparing with present in China. They are unique and special in the world (Chen et al., 1990; Li et al., 1988; Li et al., 1994; Li et al., 1995; Liew et al., 1998; Qin and Yu, 1998; Sun et al., 1995; Wang et al., 1990; Yao et al., 1994). The palaeoclimate at 21ka BP in China has been reconstructed and the results indicated that there were very different dry and wet climate patterns in the east and the west, and a dramatically decreases in temperature in this area. But the dynamical mechanisms and atmospheric circulation background of the climate anomalies at 21ka BP are not very clear. Some experiments to reproduce this condition at 21ka BP have been conducted just for the global climate at 21ka BP (Dong



et al., 1996; Joussaume and Taylor, 1995; Kutzbach et al., 1998). But so far no good simulation results of paleoclimate experiments have been reported about the climate change in China at last glacial maximum, especially the explanations of mechanism of East Asian monsoon variations.

In this section, based on the analysis of different sources of paleoclimatological records, by using a general atmospheric circulation model (AGCM) coupled with a simplified land processes model (SSiB) (e.g. AGCM+SSiB) and the forcing conditions, climate conditions at 21ka BP in China are reproduced and the possible dynamical mechanisms are explored. By comparing reconstructed climate from various proxy indices with atmospheric circulation features from the model, the major characteristics associated with the potential mechanisms of climate change at 21ka BP in China are addressed preliminarily (Chen et al., 2000, 2001; Yu et al., 2001).

### ***Forcing conditions***

The experiments are designed according to Paleo-climate Modeling Inter-comparison Project (PMIP). It is used to determine the model predicted equilibrium climate that is consistent with certain imposed changes in boundary condition characteristics of the period under study. Here, the boundary conditions indicate various prescribed conditions (including orbital parameters which determining the insolation pattern, atmospheric CO<sub>2</sub>, glacial ice distribution and sea surface temperatures), which are considered to be external to the components of the climate system for typical GCMs. By considering equilibrium climate states, the study limits the kinds of issues that can be addressed concerning the evolution of climate from the state to another. For the last glacial maximum (LGM), two experiments are designed in PMIP. In one experiment SSTs are prescribed, while in the other experiment, SSTs are created by ocean model. In this study, the first method is used and the massive ice sheets covering North America and Scandanavia have been prescribed according to reconstruction by Peltier (1994). It is very important that the last glacial maximum climate is characterized by large changes in the surface boundary conditions (ice sheet extent and elevation, sea surface temperatures (SSTs), and surface albedo) and atmospheric carbon dioxide concentration, but only minor changes in the insolation pattern. This period (21ka BP) is very important for understanding how ice sheets and lowered CO<sub>2</sub> levels influence the climate. Among the climate features of interest in this experiment are only the simulated changes in the Northern Hemisphere jet stream location and associated changes in the storm tracks (Gates, 1976; Valdes and Hall, 1994; Manabe and Broccoli, 1985; Rind, 1987; Kutzbach and Guetter,

1993; Joussamue, 1993). To our knowledge, there is no numerical simulation study focusing on Asia monsoon climate features in China at 21ka BP. Therefore, in this study, we design the experiment and attempt to simulate the climate at 21ka BP in East Asia and China.

**Design of simulation**

In this experiment 21ka BP simulation is driven by two kinds of forcing conditions. One is associated with solar radiation, e.g. earth orbital parameters (perihelion, eccentricity and obliquity). The other is associated with the earth surface conditions, including sea surface temperatures (SSTs), snow and ice coverage, atmospheric CO<sub>2</sub> concentration and vegetation. In order to identify the climate change at 21ka BP from the present, we run both 0ka and 21ka BP experiments. In the 0ka (control) test, SST is present data with 10-year variation. Snow and sea ice coverage with seasonal variation, vegetation distribution and earth orbital parameters are same as present. CO<sub>2</sub> concentration is 280ppm. In the 21ka BP experiment, SSTs, sea ice, snow cover and ice sheet are determined based on PMIP document. CO<sub>2</sub> concentration is 200ppm, and earth orbital parameters are estimated according to Berger (1978). Some researches indicated that interaction between vegetation and atmosphere is very important in climate simulation (Foley et al., 1994; Martin et al., 1999; Winkler and Wang, 1993). In this study vegetation distribution at 21ka in Eastern Asia are prescribed according to pollen data (Yu et al., 2000). All forcing conditions are summarized in Table 2.3. For both 21ka BP and control experiments, 11 modeling years simulation was run, and averages of last 10 years were treated as mean equilibrium climate conditions. Here, 10-year average is used as a typical period of climate status at 21ka BP and to be compared with modern climate.

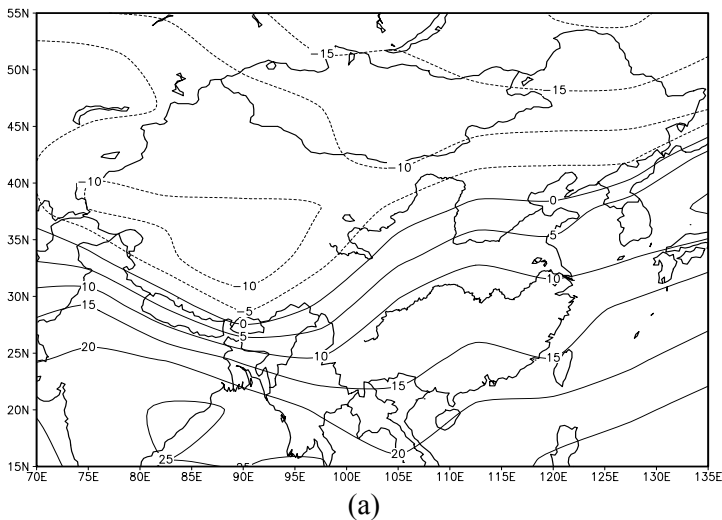
Table 2.3 Earth orbital parameters and boundary conditions for simulation experiments

Parameters	The earth orbital parameters			Boundary conditions
	Eccentricity	Perihelion	Obliquity	
Present (0ka)	0.0167	282.04	23.446	280ppm CO <sub>2</sub> concentration, 10-year SST, present snow and sea ice cover, present vegetation distribution
21ka BP	0.0187	294.42	22.949	200ppm CO <sub>2</sub> concentration, SST from CLIMAP, snow and ice sheet from PMIP, vegetation distribution changed over Eurasia from geological data

### Simulation Results

#### (1) Modeled climate features at 21ka BP in China

The simulated surface temperature, precipitation and effective precipitation P-E at 21ka in the area of China are shown in Fig.2.11 (a), (b) and (c). The annual mean surface temperatures (shown in Fig.2.11(a)) are from 20°C to -20°C with the region from Hainan Island, southern China, to northeastern China. Annual mean surface temperature in Tibetan Plateau is about -5°C to -10°C, the one of the coldest regions by the model simulation, and the another one is northeastern China. It can be seen from Fig.2.11 (b) that there is high annual precipitation in the Tibetan Plateau region. The maximum of that is more than 2.5mm/d, and the most of the Plateau is covered by area of 1.5mm/d. There is the region covered by 2.5mm/d in the north of China. On the contrary, precipitation in eastern and southeastern China is less than 2.5mm/d. Index representing dry and wet conditions (annual effective precipitation P-E), is mapped in Fig.2.11 (c). The pattern of P-E distribution is very similar to that of precipitation. The maximum of that is in Tibetan Plateau. In the middle and south of the Plateau, P-E is greater than 1.5mm/d, and maximum is about 2mm/d. As a contrast, P-E is less than 1mm/d in the eastern China, which is much less than that in the Plateau. This distribution shows that there was humid climate in Tibetan Plateau and dryer climate in the east of China at 21ka BP.



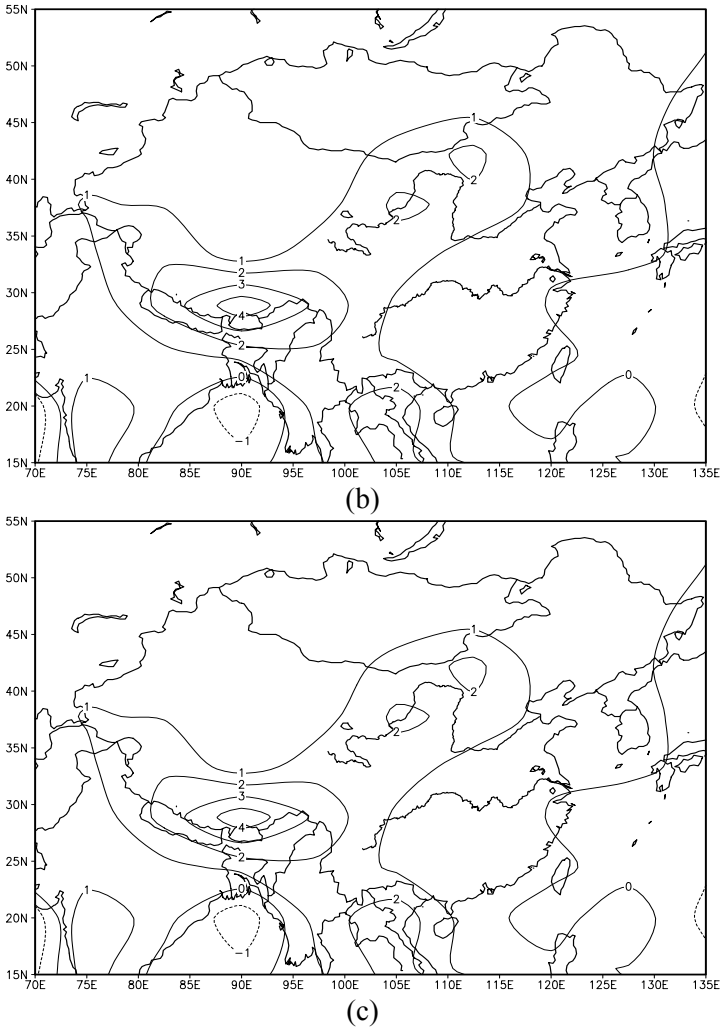
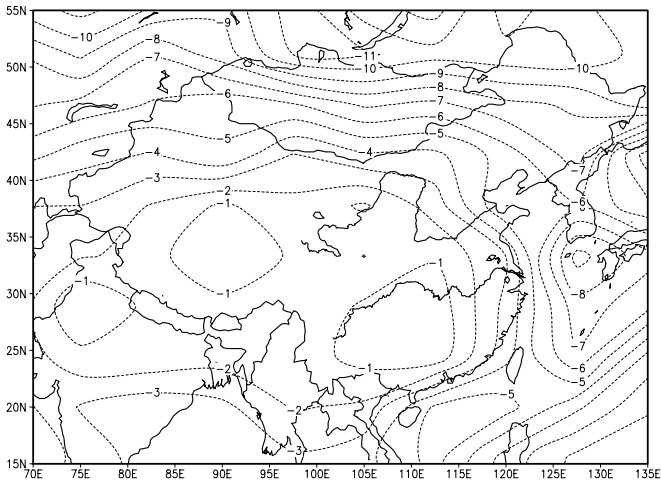


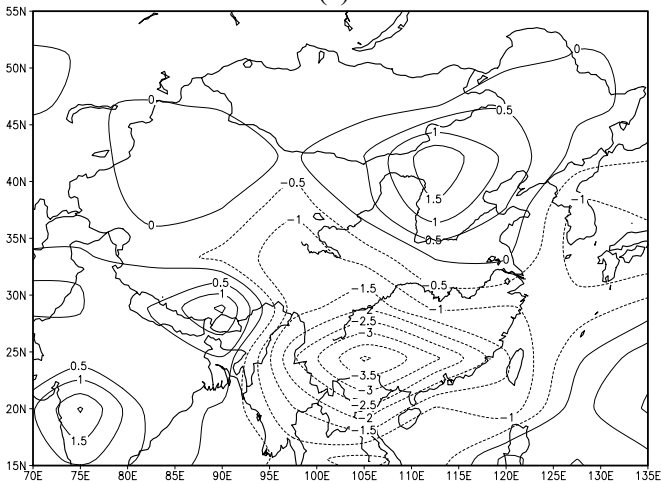
**Fig. 2.11.** Simulated surface temperature, precipitation and effective precipitation P-E at 21 ka BP (a) Annual surface temperature(°C), (b) Annual precipitation(mm d<sup>-1</sup>); (c) Annual effective precipitation P-E (mm d<sup>-1</sup>)

From above results we can find the main climate features at 21ka BP in China are that it was colder and wetter in the Tibetan Plateau and warmer and drier in eastern China compared with the Plateau. The differences of the climate between 21ka BP and present are shown in Fig.2.12 (a), (b) and (c). From the differences of annual mean temperature (Fig.2.12 (a)), it can be seen that decreases in temperature ranged between 1°C to 10°C at 21ka

BP. In the Plateau, temperature decreasing in summer is less than that in winter. This indicates that climate was warm in summer half year in Tibetan Plateau. The anomalies of annual precipitation at 21ka BP (Fig.2.12 (b)) shows that the positives located at Tibetan Plateau, northwest of Xinjiang, north and northeast of China. The differences of annual precipitation are negative in the regions where precipitation is plentiful at present, such as the east and the southeast of China. Especially in the up and middle basins of Yangtze River, the decrease in precipitation is more than 1mm/day. It means that these areas are short of precipitation at 21ka BP. The distributions of difference of annual effective precipitation (P-E) are almost the same as that of annual precipitation (Fig. 2.12 (c)).



(a)



(b)

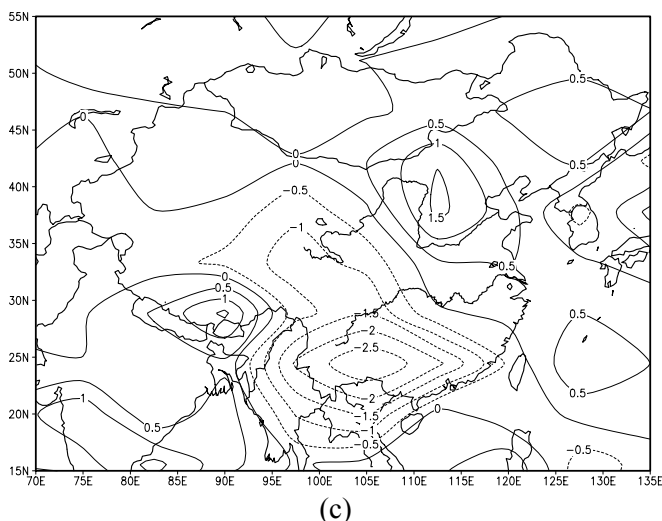


**Fig. 2.12.** Differences of simulated temperature at 21 ka BP and present (a) Difference of annual temperature (in  $^{\circ}\text{C}$ ); (b) Difference of Annual precipitation (in  $\text{mm d}^{-1}$ ); (c) Difference of Annual effective precipitation P-E (in  $\text{mm d}^{-1}$ )

From the simulation of 21ka BP conditions, we can find that it is colder in China at 21ka BP than present, and the humidity spatial patterns are almost inverse between 21ka BP and present, e.g., it is wetter in the west and drier in the east of China at 21ka BP.

## (2) Comparison between the simulation and paleoclimate evidence of 21ka BP

The simulation of climate at 21ka BP is validated by palaeoclimatical evidence. Reconstructed lake status and vegetation pattern at 21ka BP in China from paleo-lake -status database and pollen database can be used as indices of the climate conditions, are compared with the model simulation results.

The lake records show that lake-water levels are low at present in the northwest, north and northeast of China, and they are high in southern and southeastern China today. The conditions registered by lake-status match the precipitation distribution in the present China. The data of 21ka BP show high lake water levels in Tibetan Plateau and northwestern China and the low levels in the eastern China. These reconstructed climate features at 21ka BP were wet in the west and dry in the east of China. The distribution of vegetation patterns shows that the cold and humid conditions are in the northeast of China. As a comparison, modern vegetation patterns in the

southeast of China is indicating warm and wet condition, the steppe and desert vegetation responding to dry condition in the northeast and northwest of China, while the tundra in eastern Tibetan Plateau controlled by alpine cold and wet conditions. In these regions climate is colder and drier. While at 21 ka BP in China, the vegetation in the most eastern China, except for the coastal zone of southeast, was characterized by the steppe and deserts. There were some vegetation adjusting to humid climate in Tibetan Plateau and the northeast of China. Therefore the climate in these regions was cold and humid, and consistent with the distributions of modeled precipitation and effective precipitation shown in Fig.2.12.

### **Discussion**

The preliminary simulation results of climate at 21ka BP in China discussed above give the typical climate conditions that have been addressed by a lot of geological data. The simulation of AGCM+SSiB model to climate at 21ka BP in China is fare consistent with reconstructed paleoclimate. Before then there were some simulation experiments by using CCMs and UGAMP, but these experiments could not give realistic Eastern Asia monsoon system signal and precipitation field. In our study, modeled Eastern Asia monsoon system is better and 21ka BP simulation is agreed with geological evidences.

Based on the comparison between model output and data analysis, we can obtain preliminary conclusions as follows:

(1) The modeled results of AGCM+SSiB with 21ka BP boundary conditions and changed vegetation distribution experiment simulated complete different conditions at 21ka BP from the present in China, as dry conditions in the eastern China and humid conditions in Tibetan Plateau. This result is consistent with paleoclimate evidences and it shows different climate at 21ka BP comparing with present. This is the first successful simulation that captured the climate features in China at 21ka.

(2) Decreases in temperature at 21ka BP in China were significant. The range of temperature decrease is from 1°C to 10°C.

(3) The changes of eastern Asia monsoon circulation are dramatic in summer at 21ka BP. The weaker summer monsoon is associated with the decreasing of pressure differences between land and sea, while in Tibetan Plateau summer monsoon was strengthened.

## **2.6 Summary**

In this chapter, the studies on regional paleoclimate of China by proxy

data and climate models are presented. The research results of that give a brief picture of paleoclimate in the past. The most reliable and high resolution proxy data can be used to reconstruct climate time series up to more than ten thousands years. Therefore, in the last 20ka, especially in the Holocene, the climate of China is studied more sufficient both in the proxy data analysis and in the modeling. From these results we can know and understand some features of climate change since the LGM in China. Paleoclimate records can provide a reconstructed climate in the mid-Holocene in China, on basis of studies in Quaternary sciences, paleoclimatology and paleoenvironmental sciences. Records from pollen, fossil plants and animals, paleosoils, lakes, ice cores, and the Neolithic archaeological evidences have reconstructed that annual mean temperature was higher than the present in China in the mid-Holocene.

The temperature over the last millennium simulated by the global climate model ECHO-G is used to compare with the reconstructed temperature anomalies in the eastern China. By this simulated regional climate of China, we examined the possible causes and mechanisms of the past climate changes in China. A global atmospheric circulation model (AGCM + SSiB) is also used to make sensitive simulation of LIA climate, and found that the volcanic eruption, solar constant, and vegetation changes are the key factors for the climate change in LIA. Both the reduction of solar radiation and the increase of the optic depth of stratospheric volcanic dust can result in the temperature decrease over the land surface. Two types of vegetation, modern vegetation and vegetation before the Industrialization, were used to test the sensitivity in LIA climate change. As a whole, the latter has a larger rate of natural vegetation coverage than that of the former. The result indicates that the change of vegetation field engenders different tendency in temperature change, i.e. the annual mean temperature increased in East Asia, while that decreased in North Africa. Thus the promotion of the vegetation rate profits the increase of temperature, and the decrease of vegetation rate contributes to the decrease of land temperature.

Simulations suggested that increased solar radiation in the mid-Holocene played a major role in global warming, and increases of regional precipitation were mainly controlled by feedback of vegetation forcing. The comparison of simulation experiments shows that variation of the surface albedo due to vegetation change can produce the seasonal change in the thermal differences between land surface in the Eastern Asia and sea surface over western Pacific Ocean in the mid-Holocene. The forest extending in high latitude regions increased the thermal capacity of the land surface and reduced the cooling effects. As a result, the winter monsoon circulation was weakened and cold air activities were reduced, and leading to an increased winter temperature.



The model simulation shows that the main climate features at 21ka BP in China was colder and wetter in the Tibetan Plateau and warmer and drier in eastern China compared with the Plateau. The differences of annual precipitation are negative in the regions where precipitation is plentiful at present, such as the east and the southeast of China. It means that these areas are short of precipitation at 21ka BP, especially in the upper and middle reaches of Yangtze River. The simulation results are validated by lake-status of 21ka BP that shows high lake water levels in Tibetan Plateau and northwestern China and the low levels in the eastern China. That means wet climate in the west and dry in the east of China at 21ka BP.

Proxy data studies and climate modeling studies can help us understand the mechanisms of paleoclimate changes in China in great details. Also, these studies provide us an opportunity to link the climate changes in China to those in the rest of the world.

## References

- An Zhisheng, Wu Xihao, Lu Yanchou et al. (1990) A preliminary study on the paleoenvironment change of China during the last 20,000 years, Loess, Quaternary geology and global change (Part II) (in Chinese) (ed. Liu Dongsheng), Beijing: Science Press, 1-26.
- Berger, AL (1978) Long-term variations of daily insolation and Quaternary climatic changes, *J. Atmos. Sci.*, 35: 2362-2367.
- Bonan, GB, Pollard, D, Thompson, SL (1992) Effects of boreal forest vegetation on global climate, *Nature*, 359: 716-718.
- Cao JT, Wang SM, Shen J (2000) Primary study of paleoclimate changes during the past millennium in Daihai lake, Inner-Mongolia, *Marine Geology & Quaternary Geology*, 20(2), 15-20 (in Chinese)
- Central Meteorological Institute of Chinese Meteorological Administration et al., (eds), 1981: The Drought and flood Charts in China for the Last 500 years. China Atlas Press, Beijing, 332 pp
- Chen JY (1988) Preliminary studies to the several questions about lichen of glacier change in the Holocene in Wulumuqi River of Tianshan Mountain. *Science in China*, (1), 95-104
- Chen K, Bower J, Kelts K (1990) Changes in climate on Qinghai-Xizang plateau during the last 40000 years, *Quaternary Sciences*, (1): 21-30.
- Chen Xing, Yu Ge, Liu Jian (2000) A preliminary simulation of climate at 21 ka BP in China, *Journal of Lake Sciences* (in Chinese), 12(2): 154-164.
- Chen, X. et al. (2001) An AGCM+SSiB simulating changes in paleomonsoon climate at 21ka in China. *Acta Meteorologica Sinica*, 15(3): 333.
- Chen, X. et al. (2002) Mid-Holocene climate simulation and discussion on the mechanism on temperature change. *Science in China* (in Chinese), 32(4): 335.

- Chen Xing, Liu Jian, Wang Sumin (2002) Climate simulation of Little Ice Age over eastern Asia, *SCIENTIA METEOROLOGICA SINICA*, 25(1): 1-8
- Claussen, M (1996) Variability of global biome patterns as a function of initial and boundary conditions in a climate model, *Climate Dynamics*, 12: 371-379.
- CLIMAP Members Seasonal reconstructions of the Earth's surface at the Last Glacial Maximum, Geological Society of America Map Chart Series 36. 1981
- COHMAP Members, Climatic changes of the last 18,000 years: observations and model simulations, *Science*, 1988, 241: 1043-1052.
- Cubasch U et al (1997) Simulation of the influence of solar radiation variations on the global climate with an ocean-atmosphere general circulation model. *Climate Dynamics*, 13: 757.
- Ding ZL, Yu ZW, Rutter NW et al (1994) Towards an orbital time scale for Chinese loess deposits. *Quarter. Sci. Rev.*, 13, 39-70
- Dong B, Valdes P, Hall N (1996) The changes of monsoonal climates due to earth's orbital perturbations and ice age boundary conditions, *Palaeoclimates*, 1:203-240.
- Du Naiqiu, Kong Zhaochen, Shan Fashou (1989) A preliminary investigation on the palaeoclimate and palaeoenvironment based on pollen analysis in core QH85-14C, *Acta Botanica Sinica* (in Chinese), 31: 803-814.
- Etheridge D et al (1996) Morgan natural and anthropogenic changes in atmospheric CO<sub>2</sub> over the last 1000 years from air in Antarctic ice and firn. *J. Geophys. Res.*, 101: 4115.
- Foley JA, Kutzbach JE, Coe MT et al (1994) Feedbacks between climate and boreal forests during the Holocene epoch, *Nature*, 371: 52-54.
- Gates WL (1976) The numerical simulation of ice-age climate with a global general circulation model. *J. Atmos. Sci.*, 33: 1844-1873.
- Ge QS, Zheng JY, Man ZM et al (2002) Reconstruction and analysis on the series of winter-half-year temperature changes over the past 3000 years in eastern China. *Earth Science Frontiers*, 9(1), 69-181 (in Chinese)
- Group of Experts (2002) Project of Chronology Studies on the Xia, Shang and Zhou Dynasties-Report of 1996-2000: Simplified Version. World Book Press, Beijing, pp86-88 (in Chinese)
- Harrison SP, Yu G, Tarasov P (1996) Late Quaternary lake-level records from northern Eurasia, *Quaternary Research*, 45: 138~159.
- Hong Yetang, Liu Dongsheng, Jiang Hongbo et al (2000), Evidence for solar forcing of climate variation from  $\delta^{18}\text{O}$  of peat cellulose, *Sciences in China*, series D, 43(2): 217-224.
- Jones PD, Mann ME (2004) Climate over past millennia. *Rev. Geophys.*, 42, R 2002, 1-42
- Joussaume S, Taylor KE, Braconnot JF et al (1999) Monsoon changes for 6000 years ago: Results of 18 simulations from the Paleoclimate Modeling Intercomparison Project (PMIP), *Geography Research Letters*, 26(7): 859-862.
- Joussaume S, Taylor KE, (1995) Status of the Paleoclimate Modeling Intercomparison Project (PMIP), In: *Proceedings of the First International AMIP Scientific Conference* (Monterey, California, USA, 15~19 May 1995), WCRP Report, 92: 425~430.

- Kang XC, Graumlich LJ, Sheppard P (1997) The last 1835 year Climatic changes inferred from tree-ring records in Dulan Region, Qinghai. *China Quaternary Sciences*, (1), 70-75 (in Chinese)
- Kohfeld KE, Harrison SP (2003) Glacial-interglacial changes in dust deposition on the Chinese Loess Plateau, *Quaternary Science Reviews*, 21: 1859-1878.
- Kong Zhaochen, Du Naiqiu, Zhang Yijun et al (1991) Discovery of Helicia fossil floral and sporopollen assemblage of Baohuashan in Jurong county and its climatic and botanical significance, *Quaternary Sciences* (in Chinese), 326-335.
- Kotlia BS, Bhalla MS, Sharma C et al (1997) Palaeoclimatic conditions in the upper Pleistocene and Holocene Bhimtal-Naukuchiatal lake basin in south-central Kumaum, North India, *Palaeogeography, Palaeoclimatology, Palaeoecology*, 130: 307-322.
- Kutzbach, JE, Gallimore R, Harrison SP et al (1998) Climate and biome simulation for the past 21,000 years, *Quaternary Science Reviews*, 17: 473-506.
- Kutzbach JE, Guetter PJ, Behling P et al (1993) Simulated climatic changes: Results of the COHMAP climate-model experiments, *Global Climates since the Last Glacial Maximum*, ed. Wright, Jr. H. E., Kutzbach, J. E., Webb, III. T., et al., University of Minnesota Press, Minneapolis, 24-93.
- Kutzbach JE, Guetter PJ (1986) The influence of changing orbital parameters and surface boundary conditions on climate simulation for the past 18,000 years. *J. Atmos. Sci.*, 43: 1726-1759.
- Li B, Cai B, Liang Q (1988) Sedimentary characteristics of Aiding Lake, Tulufan Basin, *Chinese Science Bulletin*, 33 (8) : 608-610.
- Li B, Li Y, Kong Z et al (1994) Environmental changes during last 20ka in the Gounongcuo Regions, Kekexili, Tibet, *Chinese Science Bulletin*, 39 (18): 1727-1728.
- Li JJ (1986) Tibetan Glacier. China Sciences Press, Beijing, pp 37-66 (in Chinese)
- Li Y, Zhang Q, Li B (1995) Ostracode and its environmental evolution during late Pleistocene in the west Tibet, In: Committee of Tibet Research of China (Editor), Collections paper for meeting of Tibetan Plateau and global changes, Beijing: Meteorology Press, pp. 52~61.
- Liew P, Kuo C, Huang S et al (1998) Vegetation change and terrestrial carbon storage in eastern Asia during the Last Glacial Maximum as indicated by a new pollen record from central Taiwan, *Global and Planetary Change*, 1998,16-17: 85-95.
- Lin XC, Yu SQ (1990) Climatic trend in China for the last 40 years. *Meteor. Monthly*, 10, 16-21 (in Chinese)
- Lin XC, Yu SQ, Tang GL (1995) Series of average air temperature over China for the last 1009year period. *Chinese J. Atmos. Sci.*, 19, 525-534 (in Chinese)
- Liu GY, Wang YX, Zhang XG (1984) Dendro-climatology of tree-ring in Qilian Mountain during the last millennium and its reflection on the glacier. *Collected Papers of Institute of Glacier and Permafrost in Lanzhou*, No. 5. pp.97-108, Chinese Science Press, Beijing (in Chinese)
- Liu Hui, Wu Guoxiong (1997) Impacts of land surface on climate of July and onset of summer monsoon: a study with an AGCM plus SSiB. *Advances in Atmospheric Sciences*, 14(3): 290-308.

- Liu H, Wu G. (1995) Description for a 9-layer Spectral Climate Model (L9R15), LASG Technical Report No. 3.
- Liu Jian, Storch H, Chen Xing, Zorita E, Zheng Jingyun, Wang Sumin (2005) Comparison of simulated and reconstructed temperature in eastern China during the last 1000 years. *Chinese Science Bulletin*, 50 (24): 2872-2877
- Liu J et al (2002) Sensitivity experiment of climate change in Eastern Asia during the Little Ice Age by changing solar radiation and volcanic dust. *Journal of Lake Science* (in Chinese), 14(2): 97.
- Lou JY, Chen CT (1997) Paleo-climatological and paleo-environmental records since 4,000 a BP in sediments of alpine lakes in Taiwan. *Science in China (D)*, 40(4), 424-461
- Man ZM, Zhang W (1996) Chapter 7. Temperature changes in eastern China since Xia and Shang Dynasties in *Climate Change in China during Historical Times*, edited by Shi Y. E. and P. Y. Zhang, pp.293-300, Shandong Science and Technology Press, Jinan (in Chinese)
- Manabe S, Broccoli AJ (1985) The influence of continental ice sheets on the climate of an ice age. *J. Geophys. Res.*, 90:2167-2190.
- Martin C, Kubatzki C, Brovkin V et al (1999) Simulation of an abrupt change in Sahara vegetation in the mid-Holocene, *Geophysical Research Letters*, 26:2037-2040
- McAvaney BJ, Bourke W, Puri K (1978) A global spectral model for simulation of the general circulation, *Journal of Atmospheric Sciences*, 35: 1557-1583.
- PAGES/IGBP, CLIVAR/WCRP. The PAGES/CLIVAR Intersection, Report of a Joint IGBP-WCRP Workshop, Venice, Italy, 1994.
- Peltier WR (1994), Ice age paleotopography, *Science*, 265: 195-201.
- Prentice IC, Guiot J, Huntley B et al (1996) Reconstructing biomes from palaeoecological data: a general method and its application to European pollen data at 0 and 6 ka, *Climate Dynamics*, 12: 185-194.
- Qin B, Yu G. (1998), Implications of lake level fluctuations at 6ka and 18ka in mainland Asia, *Global and Planetary Change*, 18: 59-72.
- Qiu SH, Chen TM, Cai LZ (eds), <sup>14</sup>C Chronological Research in China. China Science Press, 1990, Beijing, 366 pp (in Chinese)
- Qin XG, Tan M, Liu DS et al (2000) Characteristics of annual laminae gray level variations in a stalagmite from Shihua Cave, Beijing and its climatic significance (II). *Science in China (D)*. 43(5): 521-533
- Ren GY, Zhang LS (1997) Late Holocene vegetation in Maili Region, Northeast China, as inferred from a high-resolution pollen record. *Acta Botanica Sinica*, 39(4), 353-362 (in Chinese)
- Rind D (1987) Components of ice age circulation. *J. Geophys. Res.*, 92: 4241-4281.
- Ruddiman WF, Mix AC (1993) The north and equatorial Atlantic at 9000 and 6000 yr BP, *Global climates since the Last Glacial Maximum*, ed. Wright, Jr. H. E., Kutzbach, J. E., Webb, III, T., et al., University of Minnesota Press, Minneapolis, 94-124.

- Sellers PJ, Mintz Y, Sud YC et al (1986) A simple biosphere model (SiB) for use within general circulation models, *J. Atmos. Sci.*, 43: 505-531.
- Shao XM, Huang L, Lin HB *et al* (2004) Precipitation changes recorded in tree-ring data during the last millennium in Delinhe region, Qinghai, *Science in China (Series D)*, 2004, 34 (2): 145-153
- Shi YF, Kong SC (1993) The climate and environment of China during the Megathermal of the Holocene, Ocean Press, Beijing, 212pp (in Chinese)
- Shi YF, Kong SC, Wang SM et al (1992) General characteristics of climate and environment of China during the Megathermal of the Holocene. In *The Climate and Environment of China during the Megathermal of the Holocene*, edited by Shi and Kong, pp.1-18, Ocean Press, Beijing (in Chinese)
- Shi YF, Zhang PY (1996) Historical Climate Changes in China. Shandong Science and Technology Press, Jinan, 538 pp (in Chinese)
- Shi Yafeng, Li Jijun, Li Bingyuan, Qingzang Plateau bulge and environmental change in the late Cenozoic Era (in Chinese), Guangzhou: Guangdong Technical and Sciences Press, 1998, 249-295.
- Street-Perrott FA, Marchand DS, Roberts N et al (1989) Global lake-level variations from 18,000 to 0 years ago: a palaeoclimatic analysis, Washington: U.S. DOE/ER/60304-H1 TR046. U.S. Department of Energy, Technical Report, 230.
- Sun J, Ke M, Zhao J et al (1995) Vegetation and climate of the Loess Plateau in China during the late Pleistocene, *Scientia Geologica Sinica*, Supplementary Issue, (1): 91-103.
- Sun Lan, Wu Guoxiong, Sun Shufen (2000) Numerical simulations of effects of land surface processes on climate: implementing of SSiB in IAP/LASG AGCM L9R15 and its performace, *Acta Meteorologica Sinica* (in Chinese), 58(2): 179-193.
- Tan M, Liu TS, Hou JZ et al (2003) Cyclic rapid warming on centennial-scale reveals by a 2650-year stalagmite record of warm season temperature. *Geophys. Res. Lett.*, 30(12), 19-1-4
- Tang Mocang, Guo Weidong (2000) The Great Ice Age cycles associated with the variation of the atmospheric heat engine efficiency, *Sciences in China, Series D*, 43(3): 284-288.
- TEMPO Members (1996) Potential role of vegetation feedback in the climate sensitivity of high-latitude regions: A case study at 6000 years B.P., *Global Biogeochemical Cycles*, 10(4): 727-736.
- Tarasov PE, Harrison SP, Saarse L et al (1994) Lake status records from the former Soviet Union and Mongolia: Data base documentation, Boulder: NOAA Palaeoclimatology Publications Series Report 2, 27.
- Tong GB, Zhang JP, Fan SX et al (1996) Environmental change at the top of Taibai Mountain, Qinling since 1ka ago. *Marine Geology & Quaternary Geology*, 16(4), 95-104 (in Chinese)
- Tu QP (1984) Trend and periodicity in air temperature variations during the last one hundred years. *J. Nanjing Institute of Meteorology*, 1984, 7: 151-161 (in Chinese)

- Valdes PJ, Hall NMJ (1994) Mid-latitude depressions during the last ice-age. In Long-Term Climate Variations - Data and Modeling. Edited by J.-C. Duplessy and M. T. Spyridakis, NATO ASI Series I, 22: 510-532.
- Wang NL, Yao TD (2002) Evidence of ice core record in Guliya on the severe cold event in early Holocene. Chinese Sci. Bull., 47 (17), 1,422-1,427
- Wang Huijun (1999) Role of vegetation and soil in the Holocene megathermal climate over China. Journal of Geophysical Research, 104(D8): 9361-9367.
- Wang SM et al (1991) Lacustrine sediments— An indicator of historical climatic variation: the case of Qinghai lake and Daihai lake. Chinese Science Bulletin, 36(16):1364.
- Wang SM (1990) The environmental change and paleoclimate in Daihai since the last ice age, Quaternary Research, (3), 223-232 (in Chinese)
- Wang SW, Zhao ZC, Chen ZH et al (1987) Drought/flood variations for the last two thousand years in China and comparison with global climatic change. In: Ye DZ et al (eds) *The Climate of China and Global Climate*, China Ocean Press, Beijing, pp.20-29
- Wang SW (1990) Trend in temperature variations in China and around the world for the last one hundred years. Meteor. Monthly, 16, 11-15 (in Chinese)
- Wang SW (1991) Reconstruction of palaeo-temperature series in China From the 1380s to the 1980s. Würzburger Geographische Arbeiten, Heft 80, 1-19
- Wang SW, Ye JL, Gong DY (1998a) Climate in China during the Little Ice Age. Quaternary Sciences, (1), 54-64 (in Chinese)
- Wang SW, Ye JL, Gong DY, Zhu JH, Yao TD (1998b) Construction of mean annual temperature series for the last hundred years in China. Quart. J. Appl. Meteor., 9, 392-401 (in Chinese)
- Wang SW, Gong DY, Ye JL, Chen ZH (2000) Seasonal precipitation series over China since 1880. Acta Geographica Sinica, 55, 281-293 (in Chinese)
- Wang SW, Zhou TJ, Cai JN et al (2004) Abrupt climate change at 4ka BP: Role of THC as indicated by a GCM experiment. Adv. Atmos. Sci., 21(2), 291-295
- Wang ZT (1991) The Little Ice Age of Northwest China. Journal of Arid Land Resources and Environment, 5(3): 64 (in Chinese)
- Winkler MG, Wang P (1993) The late-Quaternary vegetation and climate of China, In: Wright, H.E., Kutzbach, J.E., Webb, III T., et al. (Editors), *Global Climates since the Last Glacial Maximum*, Minnesota: University of Minnesota Press, pp. 221-261.
- Wright JrHE, Kutzbach JE, Webb, III T et al (1993) *Global climates since the Last Glacial Maximum*, Minneapolis, University of Minnesota Press, 468-513.
- Wu XD, Lin ZY (1981) Preliminary study of climate change of Qinghai-Tibetan Plateau during the last two thousand years. In “*Proceedings of National Conference on Climatic Change Studies*”, edited by Central Meteorological Institute, Chinese Science Press, Beijing, pp18-25 (in Chinese)
- Xia YM, Wang PF (2000) Peat record of climate change since 3,000 years in Yangmu, Mishan Region. Geographical Research, 19(1), 53-59 (in Chinese)
- Xu G.C (1997) *Climate Change in Arid and Semi-Arid Zone*. Meteorology Press, Beijing, 101 pp (in Chinese)

- Xue Yongkang, Sellers PJ, Kinter JL et al (1991) A simplified biosphere model for global climate studies, *J. Climate*, 4: 345-364.
- Yang B, Braenning A, Johnson KR et al (2002) General characteristics of temperature variation in China during the last two millennia. *Geophys. Res. Lett.*, 29(9), 38-1-4
- Yang B, Braenning A, Shi YF (2003) Late Holocene temperature fluctuations on the Tibetan plateau. *Quarter. Sci. Rev.*, 22, 2335-2344
- Yang B et al (2000) Decadal climatic variations indicated by Dulan tree-ring and the comparison with temperature proxy data from other regions of China during the last 2000 years. *Scientia Geographica Sinica*(in Chinese), 20(5): 397.
- Yang XD et al (1995) Polynological evidence of climatic change during past 2000 years in middle reaches of Huaihe River. *Memoirs of Nanjing Institute of Geography and Limnology Academia Sinica*(in Chinese), 13: 20.
- Yao TD et al (1996) Variation in temperature and precipitation in the past 2000a on Xizang(Tibet) plateau-Guliya ice core record. *Science in China, Ser.D*, 39(4): 459.
- Yao TD, Xie ZC, Wu XL (1990) Little Ice Age climate record in Dande ice cap. *Science in China (B)*, (11),1, 196-1,201
- Yao TD, Shi YE (1992) Climatic change of the Holocene in the ice core records of Dunde in the Qiliandhan Mountain in *The climate and Environment of China during the Megathermal of the Holocene*, edited by Shi Y. F. and S. C. Kong, Ocean Press, Beijing, pp.206-211 (in Chinese)
- Yao TD, Yang ZH, Huang CL (1996) Preliminary research on the climatic and environmental changes by using of the 2ka Guliya ice core data. *China Science Bulletin*, 41, 1103-1106
- Yao T, Jiao K, Zhang X (1994) Climatic and environmental records from Guliya cap, *China Science (D)*, 24: 766-773.
- Yu G., Harrison SP (1995) Lake status records from Europe: Data base documentation, Boulder: NOAA Paleoclimatology Publications Series Report 3, pp. 451.
- Yu G et al (1999) Lake records and LGM climate in China, *Chinese Science Bulletin*, 45(13): 1158-1164.
- Yu Ge (1998) Preliminary study on pollen-based biomization and Chinese biome mapping of 6000 a BP, *Acta Botanica Sinica* (in Chinese), 40(7): 665-674.
- Yu Ge, Chen Xing, Liu Jian et al (2001) Preliminary study on LGM climate simulation and the diagnosis for East Asia, *Chinese Science Bulletin*, 46(5): 364-368.
- Yu G., Harrison S.P., Xue B, (2001a) Lake Status Records from China. Data Base Documentation. Technical Report in Max-Planck-Institute for Biogeochemistry, No.4 Jena. Germany, pp 243.
- Yu G., Xue B, Liu J et al (2001b) Lake Records in China and the Palaeoclimate Dynamics. *China Meteorological Press*, Beijing, pp 196 (in Chinese)
- Yu Ge, Chen Xudong, Ni Jian et al (2000) Palaeovegetation of China: a pollen data-based synthesis for the mid-Holocene and last glacial maximum, *Journal of Biogeography*, 27: 635-664.

- Zhang De'er and Zhu SL (1981) Preliminary analysis of winter temperature conditions of south China during the last 500 years. In *Proceedings of National Conference of Climate Change*, edited by Weather and Climate Institute, Science Press, Beijing, pp.64-70 (in Chinese)
- Zhang De' er (1994) Evidence for the existence of the Medieval Warm Period in China. *Climatic Change*, 26 (2-3), 289-297
- Zhang DE et al (1998) Paleoclimate inferred from the Chinese historical records of the northern boundary of migratory locust. *Quaternary Sciences*, 1: 12 (in Chinese)
- Zhang DE (1995) Paleoclimate and environmental records available from Chinese historical documents. In: *Proceedings of the 1995 Nagoya IGBP-PAGES/PEP-II Symposium*. Nagoya: Nagoya University, 20.
- Zhang DE, Liu CZ, Jiang JM (1997) Reconstruction of wetness series of six regions in east China during the last 1000 years and abrupt climate change. *China Quaternary Research*, (1), 1-11 (in Chinese)
- Zhang LS, Fang XC, Ren GY (2000) *Global Change*, High-education Press, Beijing, 341 pp (in Chinese)
- Zhang Lansheng (1993) Study on historical change and law of subsisting environment in China (Part I), Ocean Press, Beijing (in Chinese)
- Zhang PY, Kong SC, Gong GF et al (1996), *Climate change in China during the Historical Times*. Shandon Science and Technology Press, Jinan, 533 pp (in Chinese)
- Zhang PY et al (1994) The stages of climate change in recent 2000 years. *Science in China, Ser.B*, 24(9): 998.
- Zhang, W.Q. et al (2000) The Little Ice Age and its environmental effects in the tropical zone of China. *Acta Geography Sinica*( in Chinese), 55(6): 744.
- Zhang XG, Li XQ (1982) Some characteristics of temperature variation in China in the present century. *Acta. Meteor. Sinica*, 40: 198-208 (in Chinese)
- Zhang XH et al (2000) IAP Global Ocean-Atmosphere-Land System Model. Beijing: Science Press, 8-50.
- Zhang Y, Wang WC (1993) Air temperature field near the ground in mid-Holocene in China. In Zhang Y. et al (eds) *Climate Change and its Impact*, pp91-107, Meteorology Press, Beijing (in Chinese)
- Zhang ZK et al (1999) Climatic changes of Little Ice age and its social effects in China. *Exploration of Nature*(in Chinese), 18(1): 66.
- Zhang ZK et al (2000) Lacustrine records of climatic change and human activities in the catchment of Erhai lake, Yunnan Province since the past 1800 years. *Journal of Lake Science*(in Chinese), 2(4): 297.
- Zheng JY et al (1993) An analysis on cold/wet in Shandong Province during historical times. *Acta Geographica Sinica*(in Chinese), 48(4): 348.
- Zhong K (1997) The lacustrine sediment records of the environmental changes since the Little Ice Age (LIA) in the northern parts of East Xingjian. *Journal of Xingjiang University, Natural Science Edition*(in Chinese), 14(2): 78.
- Zhu KZ (1972) Preliminary study on the climate change in China during the last 5000 years. *Acta Archeological Sinica*, 2(1), 15-38 (in Chinese)
- Zhu KZ (1973) Preliminary study on the climatic fluctuations during the last 5000 years in China. *Scientia Sinica*, 16(2): 226.



Regional Climate Studies of China

Fu, C.; Jiang, Z.; Guan, Z.; He, J.; Guo, W. (Eds.)

2008, XVII, 476 p., Hardcover

ISBN: 978-3-540-79241-3